QUANTITATIVE COMPUTED TOMOGRAPHY ANALYSIS OF PATELLAR SUBCHONDRAL BONE DENSITY

A Thesis Submitted to the College of

Graduate Studies and Research

In Partial Fulfillment of the Requirements

For the Degree of Masters of Science

In the Division of Biomedical Engineering

University of Saskatchewan

Saskatoon

By

WADENA DELSIE BURNETT

PERMISSION TO USE

In presenting this thesis in partial fulfilment of the requirements for a Postgraduate degree from the University of Saskatchewan, I agree that the Libraries of this University may make it freely available for inspection. I further agree that permission for copying of this thesis in any manner, in whole or in part, for scholarly purposes may be granted by the professor or professors who supervised my thesis work or, in their absence, by the Head of the Department or the Dean of the College in which my thesis work was done. It is understood that any copying or publication or use of this thesis or parts thereof for financial gain shall not be allowed without my written permission. It is also understood that due recognition shall be given to me and to the University of Saskatchewan in any scholarly use which may be made of any material in my thesis.

Requests for permission to copy or to make other use of material in this thesis in whole or part should be addressed to:

Head of the Division of Biomedical Engineering
University of Saskatchewan
Saskatoon, Saskatchewan S7N 5A9

ABSTRACT

Osteoarthritis (OA) is a debilitating disease marked by changes in cartilage and subchondral bone, but symptomatically marked by pain. Pain pathophysiology is poorly understood, but as patellar subchondral bone is innervated, it could be linked to OA-related knee pain. Also, subchondral cortical and trabecular bone may each play individual roles in OA-related pain pathophysiology.

The overall goal of this study was to determine how subchondral bone is related to pain in OA. The objectives of this study were 1) to measure to *in vivo* precision of computed tomography topographic mapping of subchondral density (CT-TOMASD) in the patella, and to 2) to apply CT-TOMASD to a clinical sample to determine if there were differences in patellar subchondral bone density between knee OA patients with different pain experiences.

In vivo precision ($CV\%_{RMS}$) of CT-TOMSAD in the patella ranged from 1.1% to 6.8%. Precision errors were approximately 4 times greater than observed BMD differences between healthy and OA groups.

In the clinical analysis, participants with ‘severe pain at rest’ had 16% lower BMD over the total lateral patellar facet at depths of 5-7.5mm from the subchondral surface than participants with ‘non-severe pain at rest’. Regional analysis showed that participants with ‘severe pain at rest’ had lower BMD in the inferior lateral facet; 13% at the 0-2.5mm depth, 23% at the 2.5-5mm depth, and 22% at the 5-7.5mm depth.

This is the first study to report QCT-based subchondral cortical and trabecular BMD values in the patella. This is also the first application of CT-TOMASD to a sample of participants with clinically diagnosed OA; and the first study to report relationships between BMD and pain, showing that trabecular bone changes may be related to pain.

PREFACE

Sections of this thesis have been submitted as multi-authored papers in refereed journals. CT imaging was carried out by trained technicians, and clinical diagnoses, were carried out by a participating orthopedic surgeon. The research concept and computed tomography topographic mapping of subchondral density program (CT-TOMASD) was developed by Dr. JD Johnston, and preliminary precision analysis was performed by Candace Gellert. Data analyses and manuscript preparation were carried out by myself and the co-authors contributed in editing the manuscripts for submission to refereed journals.

Submitted Papers:

1. Burnett WD, Kontulainen SA, McLennan CE, Wheaton D, Talmo C, Hunter DJ, Wilson DR, Johnston JD. Patella bone density is lower in knee osteoarthritis patients experiencing severe pain at rest. *Osteoarthritis and Cartilage.* Submitted 2012 December 15.

   Authors' contribution: Dena Burnett was jointly responsible for the original ideas behind the paper, image analyses, presentation of the findings, and writing and editing of the original paper. Dr. Saija Kontulainen assisted with statistical analyses and edited the original paper. Christine McLennan and Diane Wheaton collected participant data. Dr. Carl Talmo recruited study participants and conducted the clinical evaluations. Dr. David Hunter and Dr. David Wilson were involved in the original study design and edited the original paper. Dr. JD Johnston was responsible for the original ideas, provided supervision, and was the key editor on this paper. This research is discussed in Chapter 5 of this thesis.

   The results in this study were presented at national and international conferences:
   Canadian Orthopaedic Research Society Annual Meeting, Ottawa, ON, Canada, 2012 June 6-8. Paper No.892.
   Osteoarthritis Research Society International World Congress, Barcelona, Spain, 2012 April 26-29. Paper No. 404.

Papers in Progress:

1. Burnett WD, Kontulainen SA, McLennan CE, Hunter DJ, Wilson DA, Johnston JD. In vivo precision of computed tomography topographic mapping of subchondral density (CT-TOMASD) in osteoarthritic and normal patellae. Plan to submit to *Osteoporosis International*.

   Authors' contribution: Dena Burnett was jointly responsible for the original ideas behind the paper, image analyses, presentation of the findings, and writing and editing of the original paper. Dr. Saija Kontulainen assisted with statistical analyses and edited the original paper. Christine McLennan collected participant data. Dr. David Hunter and Dr. David Wilson were involved in the original study design and edited the original paper. Dr. JD Johnston was responsible for the original ideas, provided supervision, and was the key editor on this paper. This research is discussed in Chapter 4 of this thesis.

ACKNOWLEDGMENTS

Thank you to my supervisor, Dr. JD Johnston for providing me with an opportunity to learn, work, and grow with such a motivated, dynamic, and ambitious team. Thank you for encouraging me to "keep kicking a galloping horse" and for helping me balance this project while still letting me explore as many opportunities as I possibly could. I look forward to future work with this group and to discovering even more.

Thank you to my Advisory Committee: Dr. Mark Eramian, Dr. Sandra Webber, and Dr. Joel Lanovaz; and to my External Examiner: Dr. Paul Babyn. Your valuable feedback has helped me gain perspective on the research and scientific process.

Thank you to my co-authors for your valuable insight and feedback: Dr. Saija Kontulainen, Dr. David Hunter, Dr. David Wilson, Christine McLennan, Diane Wheaton, and Dr. Carl Talmo. Understanding that I have such an accomplished team behind me helps ease through the edits.

If it takes a village to raise a child, it takes one to raise a researcher too. Thank you to my many mentors from many backgrounds: Dr. Dolovich, Dr. Farthing, Dr. Carmalt, Dr. Fonstad, Dr. Maule, Dr. Roberge, Dr. Brad, Dr. Guo, Dr. Cooper, and Mrs. Walker. Knowing that I have a team of experts in diverse areas supporting my journey is a precious treasure.

Thank you to my research group. It's been a pleasure to work with a group with so many perspectives. I learn something new with every conversation.

Thank you to my colleagues at the Graham Centre: Prof. Rolfes, Dr. Owen, Prof. Burton, Dr. Willis, Dr. Terry, Prof. Bennetch and Dr. Moffatt. I value your encouragement and the opportunities to stretch my wings and my perspective on teaching.

Thanks to my support group in the Physics Basement and the "Wednesday Steak Day" crew. We may not have all our ducks in a row, but at least we have each other.

Thanks to Chaos and Zorro, for patiently waiting but always ready for a walk—and helping me get perspective on what's really important.

Thanks to my family, especially Auntie Brenna and Uncle Keith Stolhandske, for helping in making my trip to OARSI 2012 a reality. I made a lot of important connections and my career will only be enhanced from the experience.

Most of all, thank you Mom, Dad, Wyatt, and Chelsey. I know you shook your heads in disbelief when I decided to go "back to school" but your support means the world to me.

I would like to acknowledge funding from the Canadian Arthritis Network, the Canadian Institutes for Health Research, the College of Engineering, and the College of Graduate Studies and Research.

I’d like to dedicate my thesis to my Gramma, Eileen Newton.
Hopefully this work will help us come one step closer to fully understanding and eventually developing a cure for your “arthur-itis”.

TABLE OF CONTENTS

page

LIST OF TABLES

LIST OF FIGURES

LIST OF ABBREVIATIONS

Abbreviation	Description
2D	Two-dimensional
3D	Three-dimensional
95% CI	95% confidence interval
aBMD	Areal bone mineral density
ACL	Anterior cruciate ligament
BMD	Bone mineral density
BMI	Body mass index
BML	Bone marrow lesion
BV/TV	Bone volume fraction (bone volume/total volume)
CT	Computed tomography
CT-OAM	Computed tomography osteoabsorptiometry
CT-TOMASD	Computed tomography topographic mapping of subchondral density
CV%	Percentage coefficient of variation
DOF	Degree(s) of freedom
DXA	Dual-energy x-ray absorptiometry
FE	Finite element
HMH	Half-maximum height
HU	Houndsfield unit
ICC	Intraclass correlation coefficient
JSN	Joint space narrowing
K_2HPO_4	Dipotassium phosphate

KL	Kellgren-Lawrence
MRI	Magnetic resonance imaging
OA	Osteoarthritis
OARSI Atlas	Osteoarthritis Research Society International Atlas
PF	Patellofemoral
pQCT	Peripheral quantitative computed tomography
QCT	Quantitative computed tomography
RMS	Root mean square
ROI	Region of interest
SD	Standard deviation
TF	Tibiofemoral
vBMD	Volumetric bone mineral density
WOMAC	Western Ontario and McMaster Universities Osteoarthritis Index

GLOSSARY

Term	Definition
Anterior	Front plane of a body; referring to surface facing forward.
Areal bone mineral density	Imaging measure of bone mineral density / image area (g/cm^2) as measured by DXA
Image artifact	Any feature appearing in an image not present in the original imaged object; could be due to limitations of the imaging tool or image processing techniques.
Bone attrition	Loss of bone as measured by radiographs or flattening of articular cortical bone.
Bone marrow lesions	Region of increased signal in bone marrow on fat-suppressed T2-weighted MRI images.
Bone mineral density	General term referring to bone mass within a specified volume.
Bone volume fraction	Imaging measure of bone volume / total volume as measured by MRI.
Coronal	Plane that divides the body into anterior and posterior sections
Cortical bone	Bone tissue referring to bone of the cortex, or outer shell of bone; more dense than trabecular bone; BMD $>400mg/cm^3$.
Distal	Pertaining to the end of an extremity situated furthest from the center of a body (e.g., the distal femur is located at the patellofemoral joint).
Inferior	Bottom plane of a body; referring to the bottom surface or region.
In vivo	Latin term for “within the living”; experiment using an entire living organism.
Intraosseous	Within a bone.
Joint space narrowing	Reported change in joint space width on radiographs.
Lateral	Located at or extending to the side.
Medial	Located at or extending to the side.
Osteophyte	Bony projection that forms along the periphery of joints.

Patellofemoral joint	Joint comprised of articulating surfaces of the patella and the femur.
Posterior	Back plane of a body; referring to a surface facing rearward.
Proximal	Pertaining to the end of an extremity situated nearest to the center of a body (e.g., the proximal tibia is located at the patellofemoral joint).
Sagittal	Plane that travels from the top to the bottom of a body, dividing it into left and right portions.
Sclerosis	Region of increased bone mineral density as apparent on radiographs; stiffening or hardening of a structure.
Sesamoid bone	Bone at the apex of a joint embedded within a tendon acting to protect the tendon and increase the joint mechanical effect.
Skyline view radiograph	Weight-bearing radiograph taken with knee bent at 30° to image the patellofemoral joint space.
Subchondral bone	Bone region below cartilage.
Superior	Top plane of a body; referring to the top surface or region.
Tibiofemoral joint	Joint comprised of articulating surfaces of the tibia and the femur.
Trabecular bone	Bone tissue referring to bone with vertical or horizontal trabeculae, creating a spongy, cellular-like tissue; less dense than cortical bone; BMD < 400mg/cm^3.
Transverse	Plane that divides the body into superior and inferior sections. Also referred to as the axial plane.
Volumetric bone mineral density	Imaging measure of bone mineral density / image volume (g/cm^3) as measured by QCT.
Voxel	Volume element representing a value in three-dimensional space.

CHAPTER 1
OVERVIEW

1.1. Introduction

Osteoarthritis (OA) is a debilitating and painful disease characterized by joint surface cartilage degeneration [1-3]. Although cartilage degeneration is the most apparent characteristic of OA, changes in underlying bone immediately below cartilage (subchondral bone) have been proposed to influence and accelerate cartilage degeneration [4]. Subchondral bone changes are a prominent risk factor of OA, resulting from changes to the biomechanical loading environment within the affected joint [2, 5, 6]. Bone mineral density (BMD) is a surrogate measure of mechanical properties [2, 7] and can be measured using various imaging techniques.

Pain is the dominant symptom in OA, and is typically measured using the Western Ontario and McMaster Universities Osteoarthritis Index (WOMAC) [8]. Pain is also the primary focus of most treatment strategies [9], including prioritizing for joint replacement [10]. Unfortunately, pain may not necessarily be present in early stages of OA [11-13], making patient self-identification difficult [14]. The relationship between pain and radiographic OA is complicated as they are poorly related in mild OA, but more strongly related in severe OA [11]. In some cases radiographic OA may be present without symptoms, or vice versa where symptoms are present but without evidence of radiographic changes associated with OA [15].

The patellofemoral (PF) compartment is involved in 50% to 65% [16, 17] of clinically diagnosed OA cases and is highly likely to be related to pain [12, 18]. Subchondral bone is innervated (highly supplied with nerves) [19, 20] and could be a potential source of pain in OA [21], as opposed to aneural and insensate cartilage [22].

It may be possible to learn more about the role of subchondral bone in OA progression and identify links between subchondral bone properties, such as BMD, and OA-related symptoms, such as pain, using *in vivo* imaging. However, current imaging tools are poorly suited for analyzing three-dimensional BMD in the patella. Computed tomography topographic mapping of subchondral density (CT-TOMASD) has been recently developed by Johnston et al. [23] and used to precisely measure subchondral bone density of the proximal tibia in cadaveric [24, 25] and *in vivo* studies [26]. These early studies show the potential to use CT-TOMASD to measure subchondral bone density of other similar articulating surfaces, such as the patella.

This research assessed the potential use of CT-TOMASD in the patella by measuring the repeatability of density measures through a precision study. With repeatable density measures, CT-TOMASD was then used to measure subchondral BMD in a sample of individuals with clinically diagnosed OA. Relationships between BMD and OA-related pain at rest (using WOMAC) were evaluated.

1.**2. Scope**

Chapter 2 provides a review of literature to date. Chapter 3 includes my research questions and project objectives. Chapter 4 outlines the short-term *in vivo* precision analysis of CT-TOMASD in the patella in patients with and without OA as well as the CT-TOMASD process in detail. Chapter 5 describes our study comparing patellar BMD between participants with clinically diagnosed OA experiencing 'severe pain at rest' and 'non-severe pain at rest'. Chapter 6 reviews the conclusions of this research and offers recommendations for future studies.

CHAPTER 2
LITERATURE REVIEW

2.1 Anatomy

2.1.1. Knee Joint

The knee joint consists of three bones: the proximal tibia, the distal femur and the patella, and two distinct articulating joints: the patellofemoral (PF) joint and the tibiofemoral (TF) joint (Figure 2-1). The TF joint allows for flexion and extension of the leg. The PF joint guides the line of action of extensor muscles in the leg along the trochlear grove, maintaining a vertical force through the femur [27]. The primary area of interest for this study is the PF joint, which is affected in 50% to 65% of OA cases [16, 17].

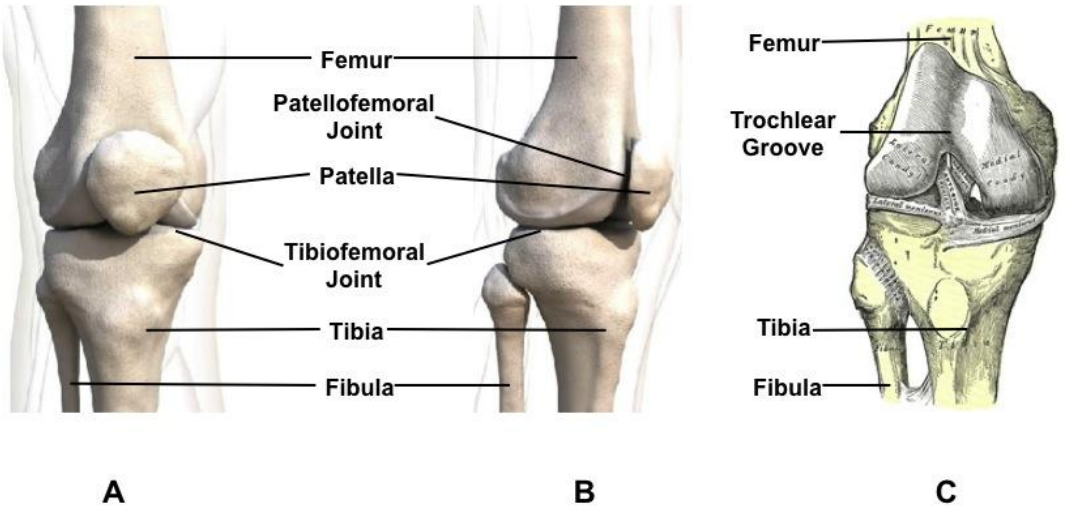

Figure 2-1. Anterior (A) and side (B) views of the knee joint, showing patellofemoral (PF) and tibiofemoral (TF) joints. Patella and quadriceps tendon removed (C) to expose trochlear groove.

2.1.2. The Patella and Patellofemoral (PF) Joint

The patella is a large sesamoid bone embedded within the quadriceps tendon that articulates in the trochlear grove on the anterior side of the distal femur. The patella acts as a fulcrum of a lever as the knee flexes and extends increasing the moment arm of the quadriceps muscle as it travels along the trochlear groove (Figure 2-1C) [28].

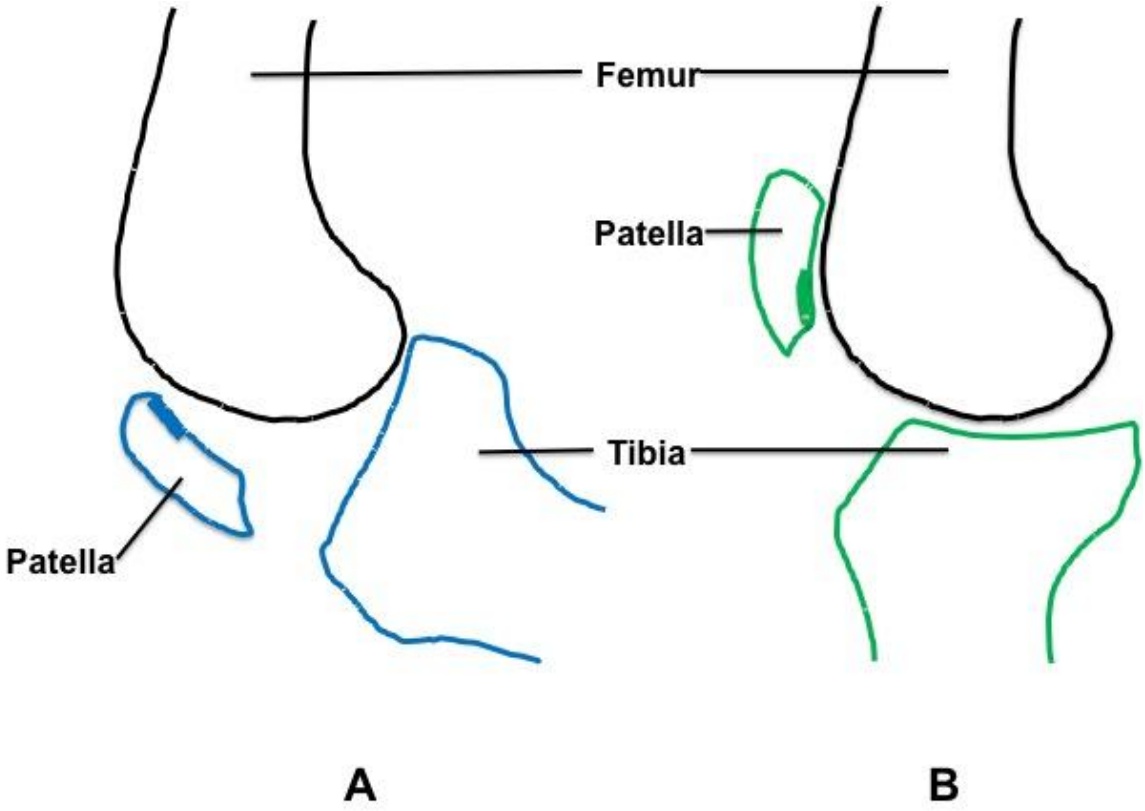

Figure 2-2. Diagram of patellar contact regions while in deep flexion (A) and in neutral alignment (B). Patella contact regions are emphasized by thickened areas.

The patella and the PF joint play an important role in force and load distribution through the knee joint, with the patella capable of sustaining loads up to eight times body weight during deep knee bends [29]. Depending on the degree of flexion in the knee, patellar surface contact regions with the distal femur will range from the superior region of the patella in deep flexion (Figure 2-2A) to the inferior region of the patella in neutral alignment (Figure 2-2B) [27].

The articulating surface (anterior face) of the patella consists of the medial and lateral facets, divided by the transverse ridge (Figure 2-3). The lateral patellar facet has 60% more force applied from the quadriceps muscles than the medial facet [30], and bears more stress (pressure) than the medial patellar facet from mid flexion to full knee extension [31].

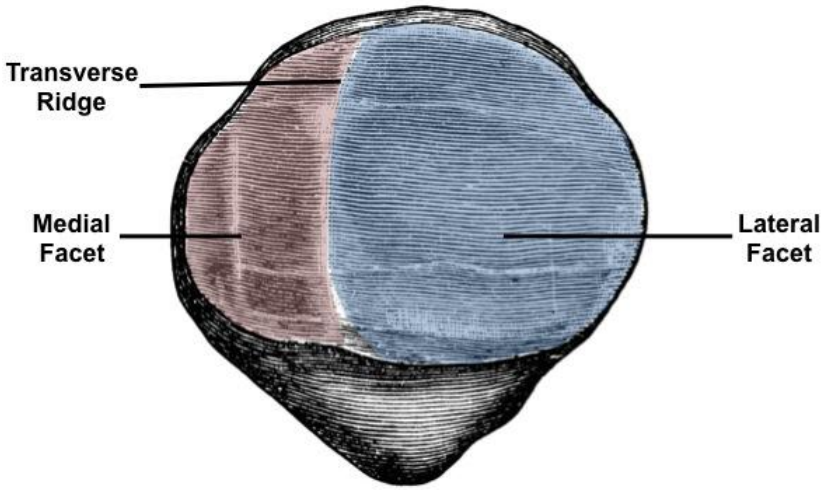

Figure 2-3. Diagram of articulating surface of the patella (lateral facet in blue, medial facet in red).

2.1.3. Articular Cartilage

The joint surfaces of each bone in the knee are covered with articular cartilage (Figure 2-4), a flexible connective tissue that serves as a low friction bearing material and allows transmission of loads between surfaces. Cartilage is avascular, aneural [19, 20], and insensate [22], therefore has a weak regeneration ability. Typical cartilage thickness in the healthy patella can range from 3mm to 5mm [32, 33].

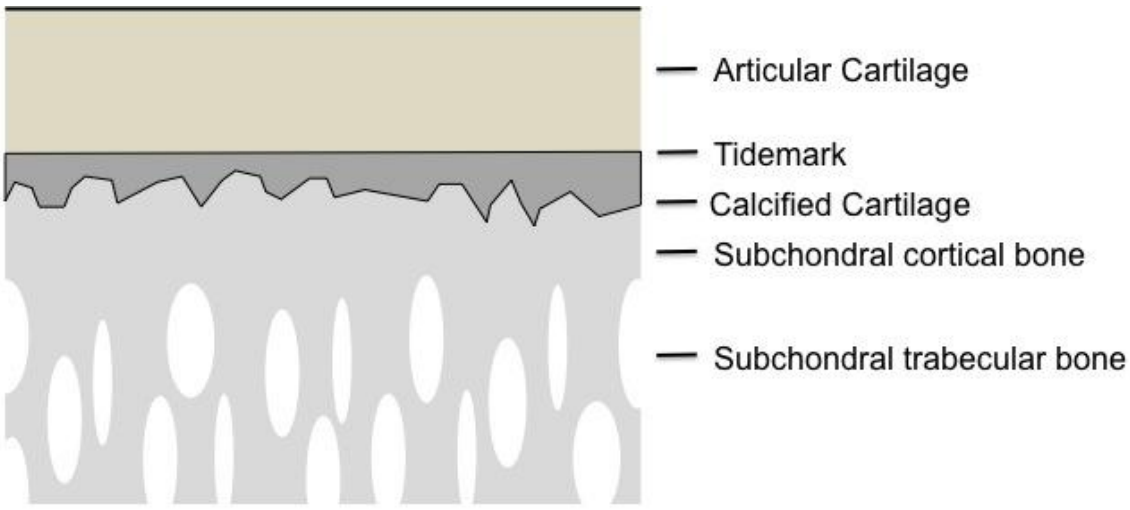

Figure 2-4. Schematic diagram of the layers in the subchondral bone region showing articular cartilage, subchondral cortical bone and subchondral trabecular bone.

2.1.4. Subchondral Bone

The region directly inferior to articular cartilage is comprised of various layers of tissues:

- tidemark; noting the division between articular cartilage and bony subchondral tissues (Figure 2-4);
- calcified cartilage; poorly mineralized tissue, ranging from 23 μm to 230μm [34], associated with subchondral cortical bone (Figure 2-4);
- subchondral cortical bone or subchondral endplate; thin highly mineralized layer of bone tissue (bone mineral density (BMD) > 400 mg/cm^3) [35] (Figure 2-4);
- subchondral trabecular bone; also known as cancellous bone, more porous tissue that acts as a support to overlying subchondral cortical bone (BMD < 400 mg/cm^3) [35] (Figure 2-4).

"Subchondral bone" is a term used to describe the subchondral structure, including subchondral cortical and subchondral trabecular bone and acts as the joint's primary supportive structure and energy-transferring source [36]. Subchondral bone and cartilage both play a role in the development and pathogenesis of OA, but distinct mechanical changes at various stages of

disease progression remain unknown. A current hypothesis in OA initiation and progression poses that as the rate of bone turnover increases, through the adaptive nature of bone modeling, the subchondral plate thickens and stiffens, disrupting the mechanical environment, leading to cartilage damage [1, 4, 37].

2.2. Osteoarthritis

Osteoarthritis affects approximately 85% of the Canadian population over 75 years of age [38], with knee OA being the most common form of clinically diagnosed OA [39]. OA is commonly thought as primarily affecting the TF joint, often overlooking the PF joint [40-42]. In the Framingham Osteoarthritis Study, radiographs from 1420 participants were evaluated with 32.9% showing evidence of radiographic OA, 15.7% showing evidence of radiographic changes leading to increased OA severity, and 9.5% showing evidence of symptomatic OA [43]. From the UK-based Knee Clinical Assessment Study, a group of 777 individuals expressing knee pain were classified based on radiographic assessment, with 68% showing no evidence of OA, 31% showing evidence of TF OA, 40% having combined (PF and TF) OA, and 24% showing only evidence of PF OA [17]. Although the TF joint tends to be the most evaluated in clinical studies [40], in this study half of the participants with OA showed evidence of radiographic OA in the PF joint.

2.2.1. Risk Factors

A wide range of research exploring OA risk factors exists, yet very little is understood about the primary "cause" of OA. Some known risk factors include systemic and biomechanical factors, such as hormonal status, bone metabolic biomarkers, joint mechanical environment, obesity, joint injury, joint alignment, age, sex, and bone mineral density (BMD) [44]. It is very likely that disease onset and progression is a result of a combination of these elements, and treatment strategies typically incorporate a variety of methods that target many risk factors [9].

Of interest to this project, multiple imaging studies have shown relationships between BMD and OA [44, 45]. Higher BMD may be associated with denser, stiffer bone, which may lead to increased mechanical stress in cartilage during joint loading, cartilage damage, and increased risk of OA [2]. A large study, once again using the Framingham OA cohort, found that

mean femoral BMD was higher in women with mild OA, but lower in women with severe OA [46]. Other studies have found similar relationships [47, 48], supporting that high BMD is associated with an increased risk of OA. Studies show that subchondral bone changes are related to cartilage degeneration [49, 50] or pain [51-54], but the relationship between disease progression and BMD is currently unknown. As BMD is related to mechanical properties [2, 7], it may be useful in understanding the relationship between disease progression and OA; BMD can also be easily monitored and measured using various imaging tools.

2.2.2. Disease Characteristics

Osteoarthritis can be characterized through clinical symptoms, morphological changes in the joint environment, or biomechanical alterations. Clinically, OA is a disease characterized by pain, joint dysfunction, limited motion, possible swelling, stiffness, and radiological evidence such as osteophyte presence (bony projection along joint margin), joint space narrowing, and sclerosis (regional bone tissue hardening) (Figure 2-5) [5, 6, 44, 55]. Morphological joint changes associated with OA may include articular cartilage loss; subchondral bone changes including sclerosis, cysts, bone marrow lesions, or attrition; osteophyte presence; and synovial inflammation [5, 37, 44, 55, 56]. Biomechanically, OA is characterized through the process of a failed repair of joint damage potentially caused by mechanical or loading changes within the joint [37, 55, 57], where changes may include altered loading patterns or changes in cartilage or subchondral bone mechanical properties (e.g., stiffness, strength, geometry).

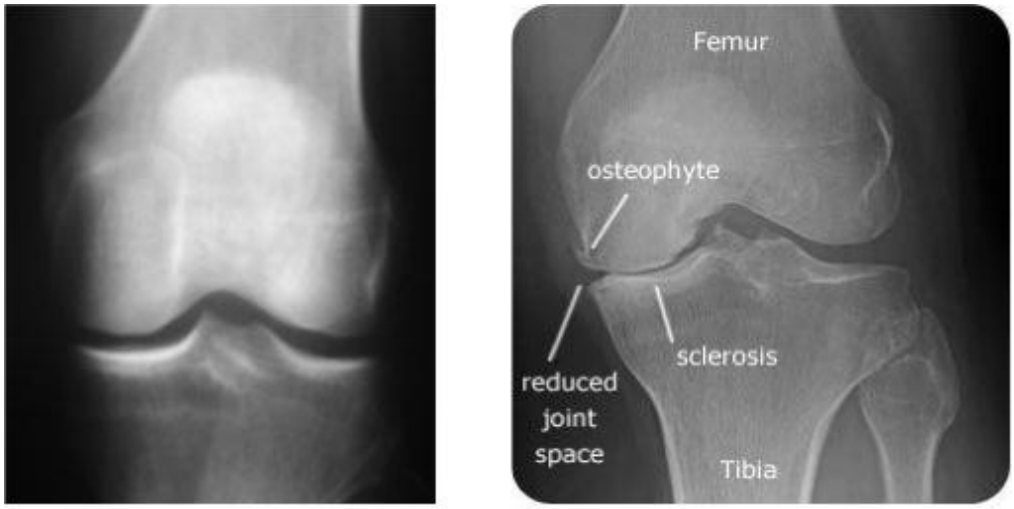

www.bjc-houston.com/hip

stemcelldoc.wordpress.com/2011/11/16/knee-osteoarthritis-grading-limitations-of-x-rays

Figure 2-5. Representative radiographs of normal (left) and OA (right) knees. Note the evidence of osteophytes, joint space narrowing and sclerosis in the OA joint on the right.

2.2.3. Clinical Classification

Clinical classification of OA can be divided into two cases: a) radiographic OA or b) symptomatic OA. Radiographic OA occurs when evidence of radiographic changes (osteophytes, joint space narrowing, sclerosis, and subchondral cysts) are present in a clinical evaluation. Symptoms (pain, stiffness, loss of function, alteration in joint shape, inflammation) may or may not be present in all cases of radiographic OA [15]; but symptomatic OA may be present in the absence of radiographic joint changes [15]. For example, in a population study of 6880 individuals, 14.6% reported symptomatic knee pain, 3.7% exhibited evidence of radiographic OA, and 25.6% reported arthritis at any joint site (Figure 2-6) [15]. Of the individuals that exhibited radiographic OA, only 47% reported clinical OA symptoms. But, in those who reported OA symptoms, only 15% showed evidence of radiographic changes. To complicate the matter, of those with self-reported OA, 11% showed evidence of radiographic changes, and 34% showed OA symptoms.

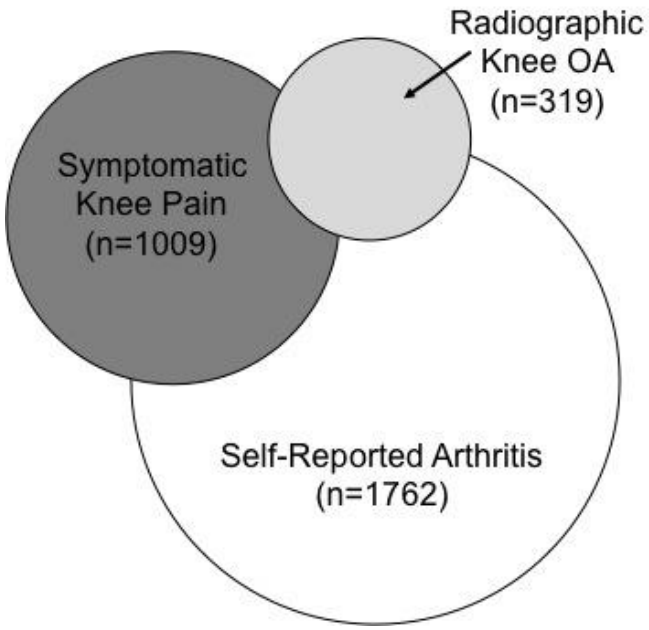

Figure 2-6. Proportions of radiographic OA, symptomatic knee pain and self-reported OA in National Health and Nutrition Examination Survey I study (adapted from Hannan 2000 [15]).

2.2.3.1. Radiographic measures

The most common clinical measure to determine radiographic knee OA severity is the Kellgren-Lawrence (KL) scoring system [58] (Table 2-1). The KL system uses qualitative and subjective radiographic evidence to assess radiographic OA severity through evidence or presence of osteophytes, joint space narrowing (JSN), sclerosis (elevation of bone density), joint deformity, and bony attrition. A knee with a score of 0 shows no radiographic indication of OA, a score of 1-2 indicates mild OA, and a score of 3-4 indicates moderate to severe OA.

Table 2-1. Kellgren-Lawrence [58] scoring system for OA severity based on radiographic evidence.

Grade	Qualifier	Radiographical features
0	None	Normal, no osteophytes, no evidence of OA
1	Doubtful	Possible osteophytic lipping
2	Minimal	Definite osteophytes, possible joint space narrowing
3	Moderate	Multiple or moderate osteophytes, definite joint space narrowing, evidence of sclerosis, possible deformity of bone ends, possible bony attrition
4	Severe	Large osteophytes, marked joint space narrowing, severe sclerosis, definite deformity of bone ends, definite bony attrition

Another lesser used technique to determine radiographic OA severity is through the use of the Osteoarthritis Research Society International Radiographic Atlas (OARSI Atlas) [59]. This scoring system uses similar qualitative evidence as the KL system, but focuses on other PF joint-specific evidence of OA such as patellar subluxation—lateral tilt as presented on a skyline radiograph. This technique provides a scoring system for a variety of radiographic signs of OA and can be used to score single specific qualities, such as only JSN or only sclerosis. This flexibility allows for multiple uses of the OARSI Atlas within a study, as joints can be qualified in different severity categories depending on evidence of different OA-related qualities. For example, a skyline PF radiograph may show evidence of moderate lateral osteophytes, scoring a grade 2, but may have severe sclerosis, scoring a grade 3. This complexity is useful for clinical studies and research where evidence of distinct characteristics of OA may be necessary.

2.2.3.2. Symptomatic measures

Common symptoms of OA are joint pain, stiffness, reduced mobility, depression, and anxiety; with the most prevalent being joint pain and stiffness [9]. Pain is the dominant symptom of OA, unique to each patient and is difficult to quantify, creating frustration from both the patient's and physician's perspectives [13]. Pain is also the primary focus of most treatment strategies [9], including joint replacement prioritization [60]. Unfortunately, pain may not necessarily be

present in early stages of OA [11, 12], thus joint degeneration may already be present within the knee before the patient seeks medical consult [14].

Pain is a subjective and patient-specific experience. A focus group evaluating chronic knee and hip pain of 28 participants showed certain themes and similarities in their pain experiences [13]. Pain was intermittent and variable, with patients expressing that pain could change from month-to-month or from day-to-day. Other similarities included pain present with function, movement, activities, or body positioning; especially at night while in bed [13].

Pain while sleeping, or nocturnal pain, is a particularly common concern among OA patients as it is most often unpredictable [61] and disturbs sleep quality, thus disturbing quality of life [62]. To relieve pain, participants most often changed sleeping position for temporary relief, but most sought relief with pain medications.

The most common questionnaire used to quantify pain is the Western Ontario and McMaster Universities Osteoarthritis Index (WOMAC) [8]. The WOMAC questionnaire [8, 63] has 24 parameters in three subsections: pain, stiffness, and physical function (Table 2-2). The pain subsection is used to quantify the patient pain experience while walking, climbing stairs, lying down, sitting, and standing. The stiffness subsection measures morning joint stiffness and stiffness occurring during the day. The more involved physical function subsection asks the patient to assess the amount of difficulty they experience when performing daily activities, e.g., walking up stairs, walking down stairs, putting on socks, bending to the floor, and rising from bed. Patient responses are based on a 5-pt Likert scale (Table 2-3) where 0 represents no pain, stiffness, or functional difficulty within the past 48 hours. Scores of 1 through 4 represent mild, moderate, severe, and extreme pain, stiffness, or difficulty respectively. Pain, stiffness, and functionality subsections can be used independently or collectively.

For specific assessment of nocturnal pain (or pain at rest), the WOMAC pain subscale can be divided into various groupings dependent on common traits: weight-bearing activities (walking and up/down stairs) and non-weight bearing activities (sitting and laying down) [64].

Table 2-2. Western Ontario and McMaster Universities Osteoarthritis Index (WOMAC) questionnaire subsections with corresponding question elements.

Subsection	Question elements
Pain	Walking, Up/down stairs, Lying in bed, Sitting, Standing
Stiffness	Morning stiffness, Stiffness later in day
Physical Function	Descending stairs, Ascending stairs, Rising from sitting, Standing, Bending to the floor, Walking on a flat surface, Getting in/out of car, Going shopping, Putting on socks or shoes, Rising from bed, Taking off socks or shoes, Lying in bed, Getting in/out of the bath, Sitting, Getting on/off the toilet, Performing heavy domestic duties, Performing light domestic duties

Table 2-3. Scoring and interpretation values of the Western Ontario and McMaster Universities Osteoarthritis Index (WOMAC).

Response	Score
None	0
Mild (or slight)	1
Moderate	2
Severe	3
Extreme	4

2.2.4. Relationships Between Clinical and Symptomatic OA

Multiple radiographic features have been related to knee pain [11, 12, 65-67]. Osteophytes in the PF joint are reported as the best radiological predictors of pain (odds ratio: 5.57, 95% confidence interval (CI): 2.72 to 11.4, $p<0.05$ [66]; and odds ratio: 2.25, 99%CI: 1.06 to 4.77, $p<0.005$ [67]). Joint space narrowing (JSN) is also reported to be significantly related OA-related pain in cases with severe to extreme OA [11, 65]. Duncan et al. [12] reported that increasing radiographic severity using KL scores is associated with increasing WOMAC pain scores. Pain and radiographic evidence are poorly related in cases with mild OA, but more strongly related in severe OA cases (odds ratio: 1.5, 95%CI: 0.9 to 2.3, $p<0.001$ for KL of 1; and odds ratio: 151,

95%CI: 43 to 526, $p<0.001$ for KL of 4 [11]), making patient self-identification difficult [14] as pain may not be present in early stages of OA even though radiographic evidence of joint changes may be present [68].

Each of these studies have found promising evidence relating knee pain and radiographic features, but with inconsistent outcomes. Individual features may be related to pain, but in the most severe cases intense pain is related to the severity score of the entire knee. This could be due to the subjective and patient-specific nature of pain, or could be due to multiple factors in OA pain pathogenesis.

2.3. OA-related Pain

The source of OA-related pain is not well understood as it could be the result of multiple factors, and likely in combination [14]. From a biological perspective, neural activity within the pain pathway is responsible for the generation, and ultimate manifestation, of joint pain. Normal joint tissues tend to be insensitive to pain, possibly because a low pain threshold would result in all normal movements to be painful [5]. Pain in OA-affected tissues could be biomechanically related and due to local changes in pain pathways, causing normal function and stimuli to become painful [5].

2.3.1. Pain Pathogenesis

OA-related pain could be due to abnormal joint biomechanics [5, 6]. One theory proposes that a major component in the OA process is an adaptation mechanism within the afflicted joint, through subchondral bone remodeling, to compensate for biomechanical abnormalities (Figure 2-7) [6]. In this model, the joint attempts to regulate abnormal biomechanics through joint remodeling and subchondral bone changes. If abnormal biomechanics are successfully controlled, the joint self-stabilizes; if abnormal biomechanics are not successfully controlled, then the joint continues to go through the bone remodeling process in an attempt to alter joint shape. Joint repair depends largely on the response and remodeling of subchondral bone; with increased bone turnover potentially increasing joint pain [6, 69].

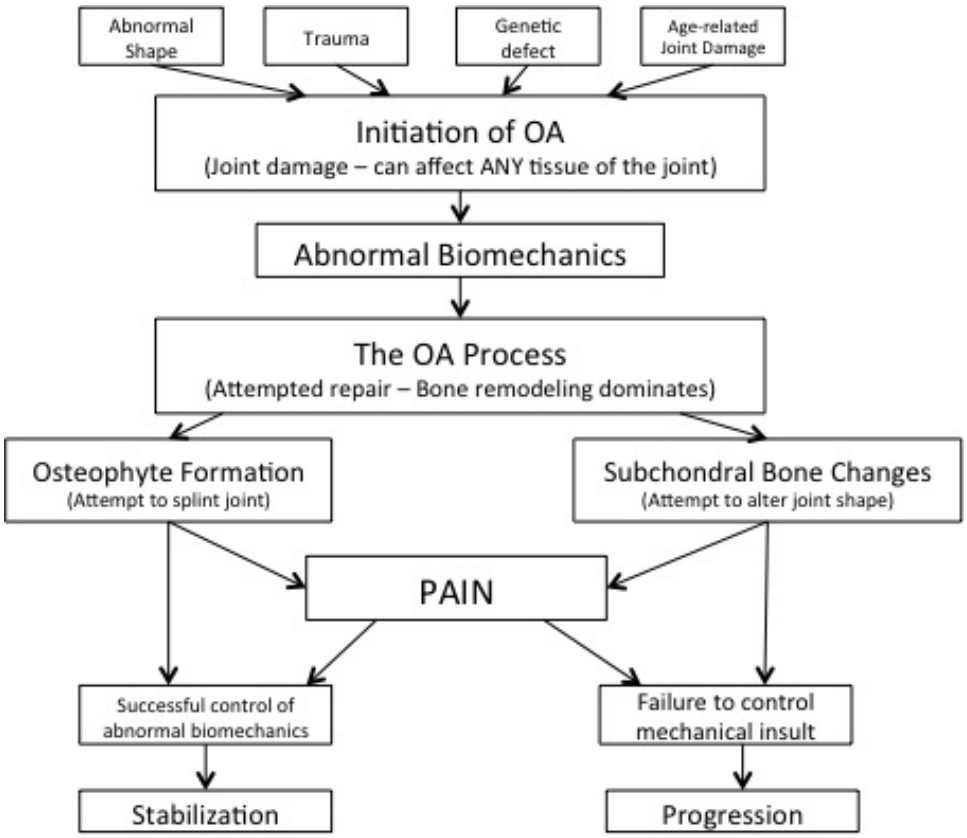

Figure 2-7. Schematic diagram of a hypothetical process of pain pathogenesis and joint remodeling, emphasizing that subchondral bone remodeling could be the primary source of OA-related pain. In this model, the joint attempts to regulate abnormal biomechanics through joint remodeling and subchondral bone changes. If abnormal biomechanics are successfully controlled, the joint self-stabilizes; if abnormal biomechanics are not successfully controlled, then the joint continues to go through bone remodeling, in an attempt to alter joint shape. Joint repair depends largely on the response and remodeling of subchondral bone; with increased bone turnover potentially increasing joint pain (adapted from Dieppe 1999 [6]).

2.3.2. PF Joint and Pain

The PF joint is strongly associated with OA-related pain [70], and even more frequently related to pain than the more explored TF joint [12]. Mild isolated PF OA is significantly associated with pain and limited joint function (combined WOMAC baseline pain score of 6.10 compared to 3.39 for mild isolated TF OA) [12]. Although the PF joint is involved in 50% to 65% of diagnosed cases of OA [16, 17], it is commonly overlooked in OA research [40]. Patellar malalignment is commonly present in patients with PF OA [71], has been identified as a risk factor for PF OA progression [41], and is commonly addressed as a site for short-term pain relief

through bracing or taping [72]. These methods may be successful in the short-term, but the reason for their success is still misunderstood, possibly due simply to a lack of investigation of the PF joint in OA.

Perhaps the primary reason for the lack of PF OA research is related to the anatomy and location of the PF joint. It is specifically difficult to acquire a comprehensive image of the PF region through the use of traditional radiographs. Clinical examination of the patella and PF region is typically through palpation [73], which can be a painful experience and does not provide a complete assessment of the PF environment as many OA-associated features (e.g., osteophytes) are not directly detectable. Standardized positioning to acquire diagnostic two-dimensional (2D) radiographs of the patella [74] are suitable for simple diagnosis, but are still limiting in that they do not offer a full representation of all surfaces, particularly articulating surfaces, of the patella.

2.3.3. Subchondral Bone and Pain

As previously mentioned, subchondral bone is densely innervated [19, 20, 22], with subchondral trabecular bone being more densely innervated than subchondral cortical bone [75]. OA-related subchondral bone changes, such as bone marrow lesions (BML), attrition, and intraosseous pressure have all shown potential correlations with pain.

2.3.3.1 Pain and bone marrow lesions

Bone marrow edemas, or bone marrow lesions (BML), are indicated by increased signal in the bone marrow on fat-suppressed T2-weighted magnetic resonance images (MRI) [76, 77] and are therefore only visible through the use of MRI. Multiple studies have shown promising relationships between BML presence and knee pain [52, 53, 77-79]; as well as BML and less mineralized subchondral tissue [80]. Although this promising evidence suggests subchondral bone is strongly related with joint pain, bone marrow lesions are dynamic and have been observed to change over time as OA progresses [50, 67, 81].

2.3.3.2. Pain and bone attrition

Another subchondral bone change associated with pain is bone attrition, defined as either loss of bone or as flattening or depression of the articular cortex [54, 82]. Current literature on bone attrition is sparse, possibly because traditional OA diagnosis is based on the opposite of attrition, i.e., based upon subchondral bone sclerosis or thickening. Two studies have found relationships between bone attrition and pain, specifically nocturnal pain, with results that were not significant but noteworthy [54, 82]. These findings showed that bone attrition was more frequent among painful knees than among knees without pain; also that attrition was present in the absence of radiographic OA. Evidence also exists relating BML to bone attrition, showing that local BMD within the BML is reduced and may compromise the local mechanical integrity of bone at the joint surface, possibly leading to attrition [80].

2.3.3.3. Pain and intraosseous pressure

A third, lesser explored, subchondral bone change associated with pain is intraosseous hypertension [83-85]. One current hypothesis is built on mechanically-based principles where, although bone volume remains constant, joint loading energy is transmitted through the cartilage and cortical layers to the trabecular bone, which serves as a series of springs accepting and distributing the loading energy [84]. Changes to the overlying cartilage and subchondral layers will compromise the energy-absorbing ability of the trabecular bone, leading to intra-trabecular tension, local intraosseous pressure changes, resulting in pain [83]. Because it is very difficult to measure intraosseous pressure without compromising the joint environment, studies investigating this hypothesis to pain are few, but promising results show that elevated intraosseous pressure is present in patients expressing pain associated with advanced OA [85].

2.3.3.4. Pain and BMD

Although not yet shown to be significantly related to pain, BMD is another subchondral bone change associated with OA and a representative measure of bone strength [86]. BMD can be precisely measured, quantified, and compared using multiple imaging modalities. Different stages of disease progression have shown varying changes and outcomes in BMD, with some

studies reporting higher BMD in patients with OA [87], and other studies reporting lower BMD [88], thus the effect of OA on BMD still remains unclear. Also, because BMD is an indirect measure of the mechanical properties of bone, the resulting changes in BMD may be joint-specific as loading patterns differ between joint surfaces, particularly in the PF joint. Studying BMD changes may help in understanding why the relationship between radiographic evidence of OA and pain is still currently misunderstood. BMD may potentially be a better predictor of OA symptoms, because it can be precisely measured and monitored before radiographic or symptomatic evidence of OA is present.

2.4. Imaging Techniques

2.4.1. Radiography

The current imaging technique to diagnose PF OA consists of standardized two-dimensional (2D) radiographs in skyline (or axial) views (Figure 2-8) [66, 74, 89, 90] as it provides the most information about the PF joint in 2D space. This radiograph must be taken in weight-bearing position with the knee flexed at 30° in order to accurately assess joint space. Although this method has been extensively validated [89], even a 2° change in x-ray tube alignment can cause an over- or under-measurement in joint space narrowing of up to 1mm. This difference in joint space measurement could change the KL score, which could lead to misclassification and mistreatment [91]. Additional radiographs, including lateral and posteroanterior views, may be helpful in identifying compartmental distribution of OA between the TF and PF joints [17].

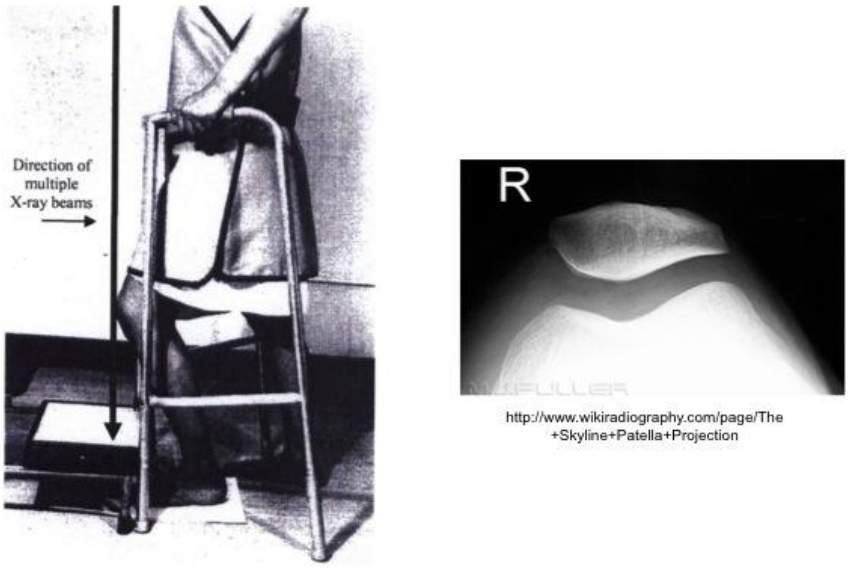

Figure 2-8. Patient positioning for standardized skyline radiographic view of patellofemoral joint (left) with resulting projection image (right). The patient places their foot on the detector film and with the aid of a support frame, bends their knee to 30°. The X-ray tube and cassette are placed directly above the patient's head [89].

Although radiographs are able to measure sizeable joint changes, it is not possible to clearly view changes in subchondral bone, such as BMD, which could be present using other imaging modalities such as dual-energy x-ray absorptiometry (DXA) [46-48, 51, 92-95], computed tomography (CT) [7, 23, 24, 26, 33, 96, 97], or magnetic resonance imaging (MRI) [7, 96, 98]. Apparent BMD as measured through these techniques is generally regarded as a surrogate measure of bone mechanical properties (e.g., stiffness, strength). Although it is possible to measure subchondral BMD with any of the listed methods, each has certain strengths and limitations, which need to be individually considered.

2.4.2. Dual-Energy X-ray Absorptiometry (DXA or DEXA)

Dual-energy X-ray absorptiometry (DXA) is a 2D projection-based imaging tool that uses photons of two different intensities to measure bone mineral attenuation, allowing for a reliable method to measure areal BMD (aBMD), or bone mineral density per unit of surface area (mg/cm^2). DXA measurements represent a three-dimensional (3D) structure as a 2D projection and are sensitive to patient positioning and subject size. If the limb of the patient is rotated in any

direction, aBMD may be altered within a region of interest (ROI). Also, larger patients will have larger bones with a larger projected surface area, thus potentially underestimating aBMD. Another limitation of DXA is the inability to separately measure subchondral cortical and subchondral trabecular BMD.

To date, DXA has not been used to determine aBMD in patellae of individuals with knee OA. However, DXA has been used to evaluate links between patellar aBMD and PF pain syndrome (pain originating from the posterior surface of the patella) [99], post-injury [100, 101], and with chondromalacia patella (softening of the undersurface of the patella) [102]. In each case, measurement technique and ROI was similar, including the entire patella in lateral view to measure aBMD (Figure 2-9). In all these studies, the affected patella had lower aBMD than the contralateral unaffected joint. Patellae in injured knees—through a ruptured anterior cruciate ligament (ACL)—had from 9.5% to 25% lower aBMD [100, 101], possibly due to inactivity or injury [100]. In patients with PF pain syndrome, affected patellae had 2.5% lower aBMD than the healthy contralateral knee [99]; and patients with chondromalacia patella had up to 6.8% lower aBMD than in the contralateral knee [102]. These studies used the contralateral knee for comparison, allowing for near equal projected surface area between affected joints and unaffected joints, nearly eliminating the concern of unequal ROI between groups and patients. A summary of these studies is presented in Table 2-4.

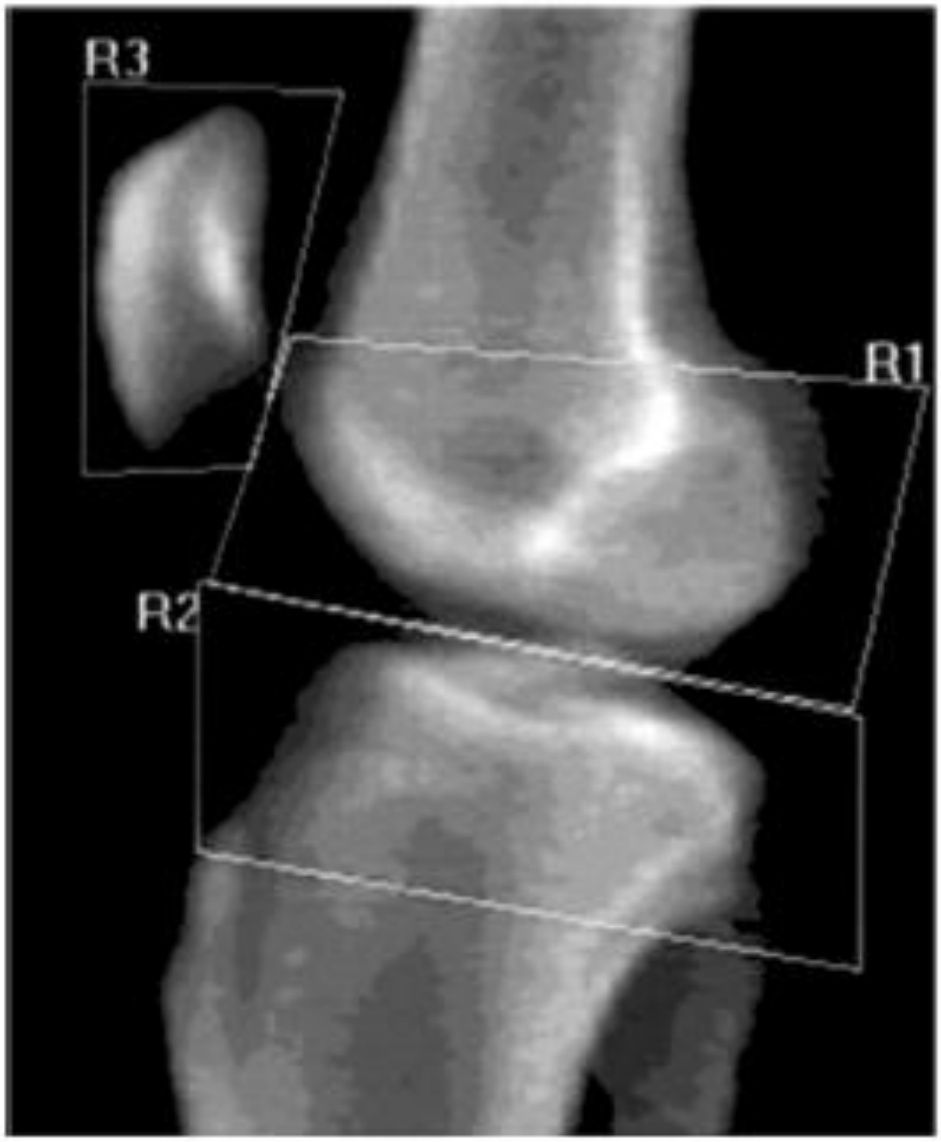

Figure 2-9. Region of interest (ROI) for studies using DXA to measure aBMD in patellae with various afflictions (R3) [100].

Table 2-4. Summary of related studies using DXA to measure patellar aBMD.

Author	Condition	# of subjects		Results				Findings	Comments
				Control		Condition			
		Control	Comparison	Mean	SD or range	Mean	SD or range		
Murphy et al. 2002	Chondromalacia patella	16*	14	1.051g/cm^2	0.896g/cm^2 to 1.266g/cm^2	0.979g/cm^2	0.763g/cm^2 to 1.77 g/cm^2	• Lower aBMD in patients with chondromalacia patella (p=0.016)	• Females only • Reduction in BMD was limited to patella.
	Chondromalacia patella	11**	11	0.969g/cm^2	0.823g/cm^2 to 1.188g/cm^2	0.906g/cm^2	0.763g/cm^2 to 1.177g/cm^2	• Lower aBMD on more symptomatic side (p=0.005)	• Females only • Reduction in BMD was limited to patella.
Leppala et al. 1998	PF pain syndrome	40**	40	1.165 g/cm^2	0.104	1.31 g/cm^2	0.092	• Lower aBMD on more symptomatic side (2.5% lower, p=0.016)	• Also found lower aBMD in distal femur (p=0.002) and proximal tibia (p=0.008)
Bayar et al. 2008	After ACL rupture	32**	32	1.195 g/cm^2	0.012	1.082 g/cm^2	0.025	• 9.46% change in aBMD. Lower on knee with injury (p<0.001)	• Found lower aBMD in distal femur and proximal tibia (p<0.001)

* Control was a healthy sample matched for age and sex.
** Control was contralateral knee.

The differences in aBMD measurements using DXA reported in these studies represent the entire patella, not localized regions or individual tissues, which may have individual roles in relation to pain. Lower aBMD in affected patellae may be a result of trabecular bone changes, but this is uncertain as DXA is not able to make a distinction between cortical bone and trabecular bone. Lower aBMD could also be due to localized changes, such as only near the subchondral surface or only near the anterior surface, but again because of the limitations of DXA and selected ROI, we do not know if the observed changes are specific to one region of the patella or if it is representative of the entire bone.

2.4.3. Magnetic Resonance Imaging (MRI)

MRI is the only imaging tool with the capability to observe changes in bone as well as surrounding soft tissues, such as cartilage. MRI offers non-ionizing radiation and 3D images. It functions by applying a series of magnetic fields to the atomic nuclei in the body, producing a rotating magnetic field detected by the scanner. However, MRI has certain limitations. First, MRI is poorly suited to measuring bone as bone is primarily composed of calcium hydroxyapatite (only having one available proton to generate a magnetic field), which produces minimal signal. Bone therefore appears as primarily black space on MRI scans, making analysis difficult. Instead, MRI can assess bone properties by indirectly imaging bone through imaging surrounding fluid, offering indirect measures of bone as a ratio of bone volume per total volume (BV/TV), a similar measure to BMD and a surrogate measure of mechanical properties [7]. This makes MRI best suited for assessing subchondral trabecular bone, as opposed to subchondral cortical bone, because there is more water-rich fluid surrounding trabecular bone than cortical bone.

To date, only one study has used MRI to assess OA and normal patellae using cadaveric specimens [96]. In these studies, a ROI was limited to a 7mm x 7mm area on each of the lateral and medial plateaus within regions of trabecular bone (Figure 2-10), omitting subchondral cortical bone was from the ROI, and from the analysis, because it produced a black MR signal. This study did not find differences in trabecular BV/TV between normal, moderate OA and severe OA patellae ($p>0.05$) [96]. A summary of these results is presented in Table 2.5.

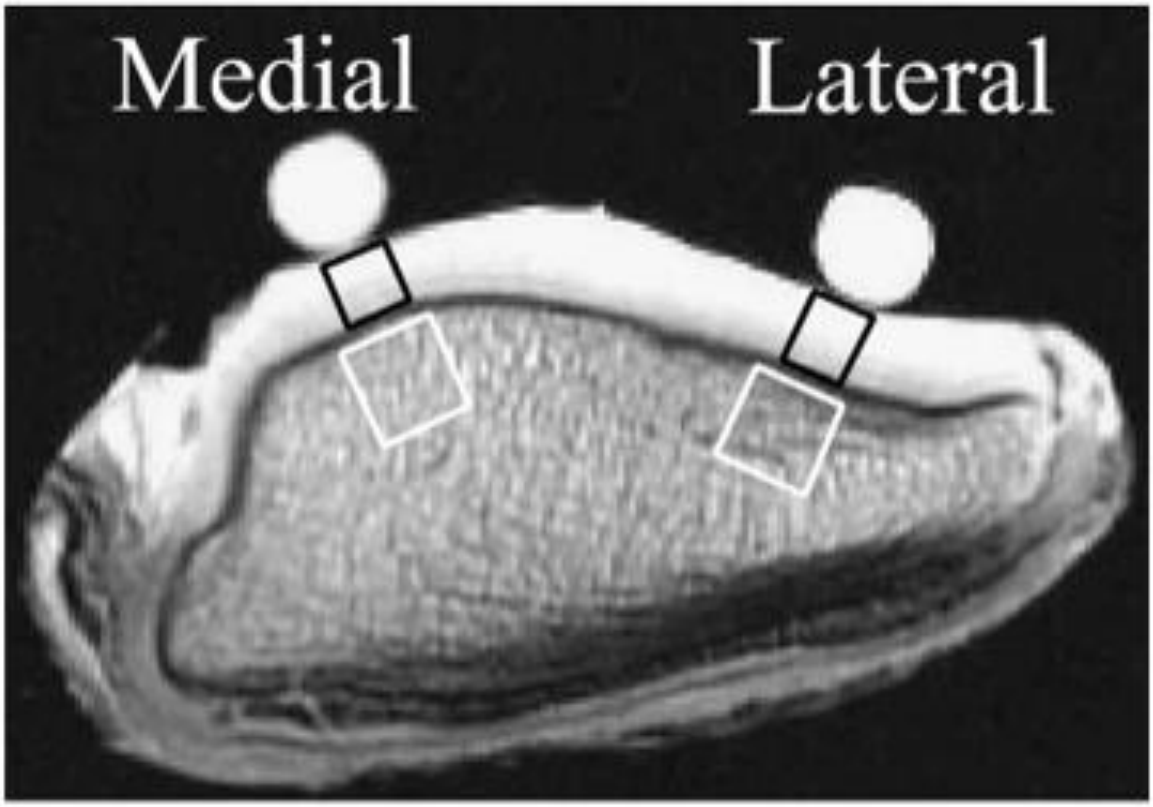

Figure 2-10. ROI in patella using MRI as assessed by Lammentausta et al. [7, 96].

2.4.4. Computed Tomography (CT)

Computed tomography is an X-ray technique that collects thin imaged "slices" of the body. Multiple images from adjacent slices can be reconstructed to create an imaged 3D volume. In quantitative computed tomography (QCT), calibrated reference phantoms are used to convert CT-acquired grayscale Hounsfield units (HU) to equivalent volumetric BMD (vBMD, mg/cm^3). These measurements provide an improved BMD measurement over DXA and are less influenced by positioning and patient size. Also, QCT is capable of differentiating between cortical and trabecular bone [103], allowing for measurements at different regions and layers within the same bone.

2.4.4.1. QCT and pQCT

Clinical QCT and peripheral QCT (pQCT) are two CT techniques applied to measure BMD in OA and normal joints.

2.4.4.2. pQCT

pQCT offers small voxel size, allowing for measurement of very small changes in BMD. However, pQCT is typically limited in a clinical setting as it is often limited to a single axial scan, such as the leg or the arm. Also, gantry sizes are typically small, limiting patellar or distal femur imaging *in vivo*.

To date, only one study [96] has used pQCT to compare BMD in cadaveric patellae without OA, with moderate OA, and with severe OA. This study used the same 7mm x 7mm ROI (only measuring subchondral trabecular bone) as the previously discussed MRI study (Figure 2-10), with a 0.5mm slice thickness and 0.200mm in-plane resolution (voxels are 0.200mm x 0.200mm x 0.5mm). Participants showing no signs of OA had significantly higher patellar trabecular BMD than those with late OA ($p<0.05$) [96]. A summary of these results is presented in Table 2-5.

Table 2-5. Summary of OA-related studies using MRI and pQCT measuring patellar BMD.

Author	Imaging type	# of subjects/specimens		Measurement	Results				Findings	Comments
					Control		Condition			
		Control	OA		Mean	SD	Mean	SD		
Lammentausta et al. 2006*	MRI	84 samples from 14 patellae		BV/TV	0.459	0.099			• Linear correlation coefficient between BV/TV and vBMD is r=0.66 (p<0.01)	• BMD varies with location • Higher vBMD in superior third
	pQCT			vBMD	387.6	101.7				
Lammentausta et al. 2007	MRI	6 (normal)	11 (moderate OA)	BV/TV	0.45**		0.46** (moderate OA)		• Linear correlation coefficient between BV/TV and vBMD is r=0.66 (p<0.01)	• Using pQCT, advanced OA had lower BMD than normal (p<0.05)
			7 (advanced OA)				0.44** (advanced OA)			
	pQCT			vBMD	400 mg/cm^{3}**		380 mg/cm^{3}** (moderate OA)			
							340 mg/cm^{3}** (advanced OA)			

* Study to determine relationships between BV/TV and BMD.
** Value estimated from figure.

Clinical QCT is more widely used than pQCT and offers many positive attributes for measuring BMD. Clinical QCT also offers small isotropic voxels (0.5-0.625mm), reducing partial volume artifacts. Scanning time is relatively short (~2.9s for hundreds of scans [23]) reducing concern for motion artifacts. Patients are exposed to ionizing radiation during a QCT scan, which may cause concern, but the knee has a low presence of radiosensitive tissues. A typical lower limb scan has a low effective dosage of ~0.15mSv [23], compared to an average of dose of 2.4mSv from annual exposure to background radiation [104] and approximately 0.05mSv during a transatlantic flight [105].

2.4.4.3. CT-based image processing

Image processing tools, such as CT-osteoabsorptiometry (CT-OAM) [33, 106, 107] and CT-topographic mapping of subchondral density (CT-TOMASD) [23, 24, 26] can be applied to QCT scans to measure BMD.

2.4.4.4. CT-OAM

CT-OAM is a CT-based imaging technique that uses maximum intensity projection image processing to select peak density within the subchondral region [106, 107]. Less dense bone above and below the peak density is ignored, and maximum density is projected to a 2D image. CT-OAM has been used in healthy patellae to measure peak density along the subchondral surface [33, 107], as well as density and strength distribution [108]. Surface distribution maps show that regions with higher density occur towards the central and superior region of the lateral facet (Figure 2-11) [33]. Unfortunately, these studies did not incorporate a calibrated reference phantom and cannot be used to reliably assess subchondral BMD in the patella. CT-OAM only provides maximum density, primarily at the subchondral cortical depth [24], and does not have the capability to perform analyses of less dense bone, such as subchondral trabecular bone.

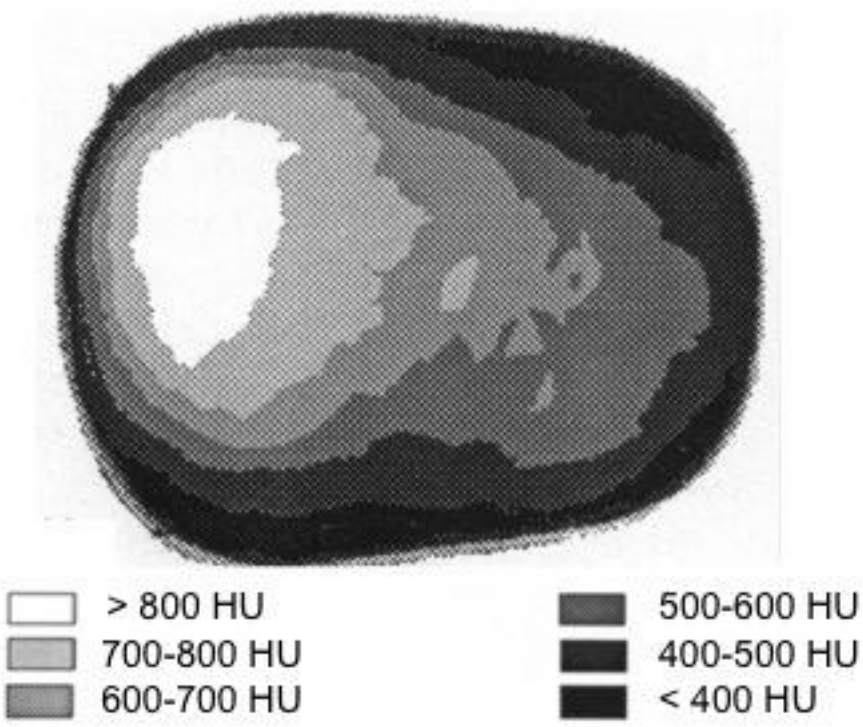

Figure 2-11. Density distribution of subchondral bone density in the patella (in Hounsfield Units (HU)) as demonstrated by CT-OAM. (Adapted from Eckstein et al. [33]).

2.4.4.5. CT-TOMASD

CT-TOMASD is a recently developed depth-specific image processing tool [23] that has been used to quantify subchondral BMD in the proximal tibia between healthy individuals and individuals with OA [24] (Figure 2-12). This imaging tool measures BMD at progressive depths from the subchondral surface (0-2.5mm, 2.5-5mm, and 5-10mm), and is able to differentiate between subchondral cortical and subchondral trabecular bone (based on BMD measurements [35]). CT-TOMASD is also capable of measuring regional BMD, as demonstrated by simultaneously measuring the anterior, central, and posterior regions of the tibial subchondral surface [23]. This method also uses isotropic voxel sizes, allowing for reformatting images in various orientations (transverse, coronal, or sagittal) without concern of stairstepping artifacts (as found when voxel dimensions are dissimilar).

CT-TOMASD also has low *in vivo* regional precision errors (<5%) in normal and OA tibiae at subchondral depths of 0-2.5mm, 2.5-5mm, and 5-10mm [26]. Therefore, this technique

has the potential to quantify regional changes in tibial subchondral cortical BMD and subchondral trabecular BMD.

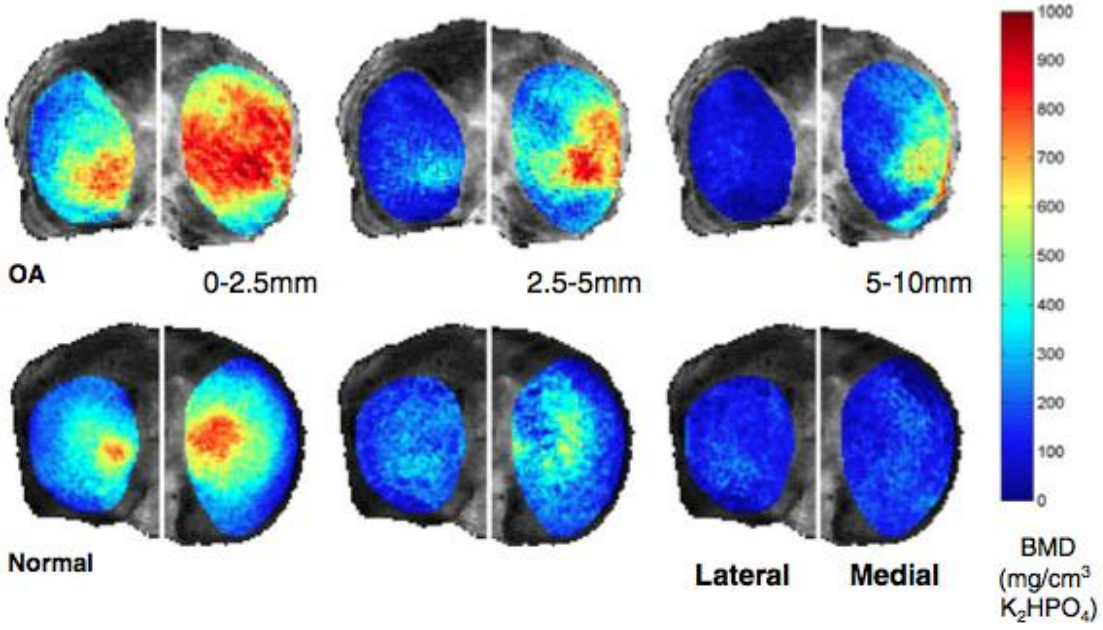

Figure 2-12. CT-TOMASD generated density maps of proximal tibial subchondral bone showing average BMD at depths of 0-2.5mm, 2.5-5mm and 5-10mm in joints with OA (top row) and healthy joints (bottom row) [26].

CT-TOMASD is an effective tool to measure regional subchondral cortical and trabecular bone in the tibia [23, 26] and shows much promise in measuring regional subchondral cortical and trabecular bone on similar low curvature surfaces, such as the patella. Preliminary regional CT-TOMASD precision errors in the patella are generally low ($CV\%_{RMS}$ of 0.8% to 7.7%) [109], showing the potential to quantify subchondral BMD in patients showing various clinical outcomes, such as different pain experiences.

2.5. Summary

1. OA is a debilitating and painful disease affecting a large proportion of the aging population. Typically, patients do not realize they are afflicted with OA until they experience pain or stiffness and the joint environment may already be biomechanically compromised.

2. PF OA is largely misunderstood due to gaps in research concerning the PF joint; however, the PF compartment is more likely related to pain.
3. Subchondral bone is largely innervated and may be related to pain progression and pathogenesis. BMD is a surrogate measure of mechanical properties in bone, and may be related to pain.
4. Some imaging tools (radiography, DXA, MRI) have certain limitations that prevent depth-specific and regional BMD analysis, especially at the patella—which is difficult to reliably image in two dimensions. Also, current imaging tools are not capable of independently measuring subchondral cortical and subchondral trabecular bone, which may have independent roles in OA pain pathogenesis.
5. CT-TOMASD has the ability to simultaneously measure subchondral cortical and trabecular BMD and may be able to measure patellar BMD.

CHAPTER 3
RESEARCH QUESTIONS AND OBJECTIVES

3.1. Research Questions

The question that motivates my research is: What role does subchondral bone play in OA-related pain? To help answer this broad question, I aimed to answer the following research questions:

1. Can CT-TOMASD provide precise *in vivo* measures of subchondral bone density in the patella?
2. Using CT-TOMASD, are there regional or depth-specific differences in patellar subchondral BMD between OA patients with differing pain experiences while at rest?

3.2. Research Objectives

To answer my research questions, my objectives were to:

1. Determine the *in vivo* precision of patellar subchondral bone density measures obtained using CT-TOMASD.
2. Identify regional and depth-specific subchondral density differences in patellae of OA patients with different pain experiences at rest.

CHAPTER 4
IN VIVO PRECISION OF CT-TOMASD MEASURES AT THE PATELLA

4.1. Synopsis

This chapter describes our testing of the *in vivo* precision of the CT-TOMASD measures in patellae with and without evidence of OA. *In vivo* precision errors ranged from 1.1% to 6.8%. This study provides evidence that the CT-TOMASD technique is suitable for analyses of subchondral bone density in the patella.

4.2. Introduction

The role of subchondral bone in knee OA progression in unclear [1, 3], particularly in the lesser-explored patella [40]. Currently, the majority of our understanding of subchondral bone changes in OA is from animal models or cadaveric studies, as opposed to *in vivo* imaging studies.

Clinically-based CT imaging tools, such as CT-TOMASD [23], have been used to precisely measure proximal tibial subchondral cortical and trabecular BMD both *ex vivo* [23, 24] and *in vivo* [26]. This technique is able to offer precise measures, with *in vivo* precision errors ($CV\%_{RMS}$) ranging from 0.9% to 3.8% using clinical CT. However, it is uncertain if the technique offers precise density measurements of other bony sites, such as the patella.

The objective of this study was to test the short-term precision of CT-TOMASD for measurements of patellar subchondral cortical and subchondral trabecular BMD in healthy individuals and individuals with OA.

4.3. Methods

4.3.1. Study Sample

Fourteen participants (3M:11F) were recruited with ages ranging from 23 to 71 years (mean ±standard deviation (SD): 49.9 ±11.9 years), including 5 left and 9 right knees. Participants were not pre-selected for presence of knee OA, but some participants informed that they were afflicted with diagnosed knee OA or undiagnosed knee pain. Left or right knees were randomly selected, unless the participant had knee pain, where the more painful knee was studied.

All knee scans were retrospectively evaluated for OA presence using the KL OA severity scoring system [58] with axial, sagittal and coronal CT reconstructions. OA severity was classified as follows:

0 Normal, no osteophytes
1 Possible osteophyte lipping
2 Definite osteophytes, possible joint space narrowing
3 Moderate or multiple osteophytes, definite joint space narrowing, some sclerosis and possible bony attrition
4 Large osteophytes, marked joint space narrowing, severe sclerosis and definite bony attrition

Of the 14 knees, seven exhibited evidence of osteophytes and sclerosis, thus were classified as OA (1M, 6F; 52.4 +/- 8.7 years; 1 with KL=1-2; 3 with KL=2; 2 with KL=3; 1 with KL=4). The remaining 7 participants showed no evidence of OA and were classified as normal (KL=0; 47.3 +/- 14.8 years). IBR approval was obtained and all participants provided informed consent prior to study involvement.

4.3.2. QCT Acquisition

Single-energy QCT was performed using a clinical CT scanner (Lightspeed 4-slice, General Electric, Milwakee, WI, USA). Participants were positioned supine with the knee of interest located in the center of the CT gantry. A solid QCT reference spine phantom (Model 3T; Mindways Software Inc, Austin, TX, USA) was located below the knee to transform grayscale CT Hounsfield units (HU) to equivalent apparent volumetric BMD (mg/cm^3 K_2HPO_4). Scanned image volumes included the distal femur, patella, and proximal tibia, but for this analysis the volume was cropped to include only images of the patella. CT scanning parameters included: 120 kVp tube voltage, 150 mA tube current, axial scanning plane, 0.625 mm isotropic voxel size (0.625 mm slice thickness, 0.625 x 0.625 mm in-plane pixel size), ~240 slices, ~90 s scan time. A standard bone kernel (BONE) was used for edge enhancement and postprocessing. Each

participant was scanned three times over two consecutive days, with a maximum of two scans per day, with repositioning between each scan.

4.3.3. CT Image Analysis

4.3.3.1. BMD conversion

From the CT images, grayscale HU were converted to equivalent volumetric BMD (mg/cm^3 K_2HPO_4) using linear regression equations developed from known reference phantom densities (r^2>0.99) (Matlab 2010b; MathWorks, Natick, MA, USA) (Figure 4-1A).

4.3.3.2. Segmentation

We segmented a set of 2D serial CT images to create a patellar 3D image volume. Each transverse plane image was segmented using a semi-automatic region growing technique with commercial software (Analyze10.0; Mayo Foundation, Rochester, MN, USA) (Figure 4-1B).

We determined subject-specific segmenting thresholds to define the subchondral bone surface by using the half maximum height method (HMH) [110, 111]. This technique uses histogram line profiles of a small region of the joint surface to define the optimum threshold value for the subchondral surface. The HMH value represents the density of a voxel with 50% cortical bone and 50% joint space and acts as a minimum value for voxels containing predominantly bone.

To perform the segmenting, a 2D seed was placed in the subchondral cortical bone region of each image using the HMH threshold value to define the boundaries for the segmented portion of the image. A stylus and an interactive touch-screen tablet (Cintiq 21uX, Wacom, Krefeld, Germany) were used for manual correction to ensure the entire patella was included within the segmented image. All pixels within the selected boundaries were included in the segmentation. The 2D segmentations were then combined and used to create a 3D volumetric object map, which was applied to the imaged patella to be rendered for boundary point selection.

4.3.3.3. Alignment

In order to minimize artifacts due to partial volume effects, CT-TOMASD surface projection analyses require the subchondral surface to be relatively flat and oriented approximately parallel with each projected image. We addressed these requirements by realigning and reconstructing the imaged patella relative to best-fit planes fit to each medial and lateral facet (Matlab). We manually selected boundary points in the axial plane (Figure 4-1C) to define the lateral and medial patellar surfaces. Fourteen boundary points were selected for each patella:

- 4 sets of 3 points defining the lateral edge, the transverse ridge, and the medial edge at equal increments long the surface of the patella, and
- 2 points defining the most superior and most inferior points along the transverse ridge.

Patellar surfaces were reoriented relative to the "best-fit" plane passing through the selected boundary points (defined using singular valued decomposition) (Figure 4-1D).

4.3.3.4. Surface projection

CT-TOMASD analysis was performed across three layers (0-2.5mm, 2.5-5mm and 5-7.5mm) measured in relation to depth form the subchondral surface (Matlab 2010a) (Figure 4-1E). Average density was projected to a 2D image to create a rendered image of 3D subchondral BMD. We then fit natural cubic splines (Matlab 2010a) to the previously selected boundary points to define the edges of the lateral and medial facets.

4.3.3.5. Normalization

Because patella size may differ between participants, analysis depth was normalized and controlled according to subchondral bone surface area and subject-specific patellar volume [23]. This process corrects for potentially shallow measurements in large patellae, and potentially excessively deep measurements in small patellae (e.g., a 2.5mm normalized depth may be an actual measurement of 2.6mm in large patellae and 2.4mm in smaller patellae).

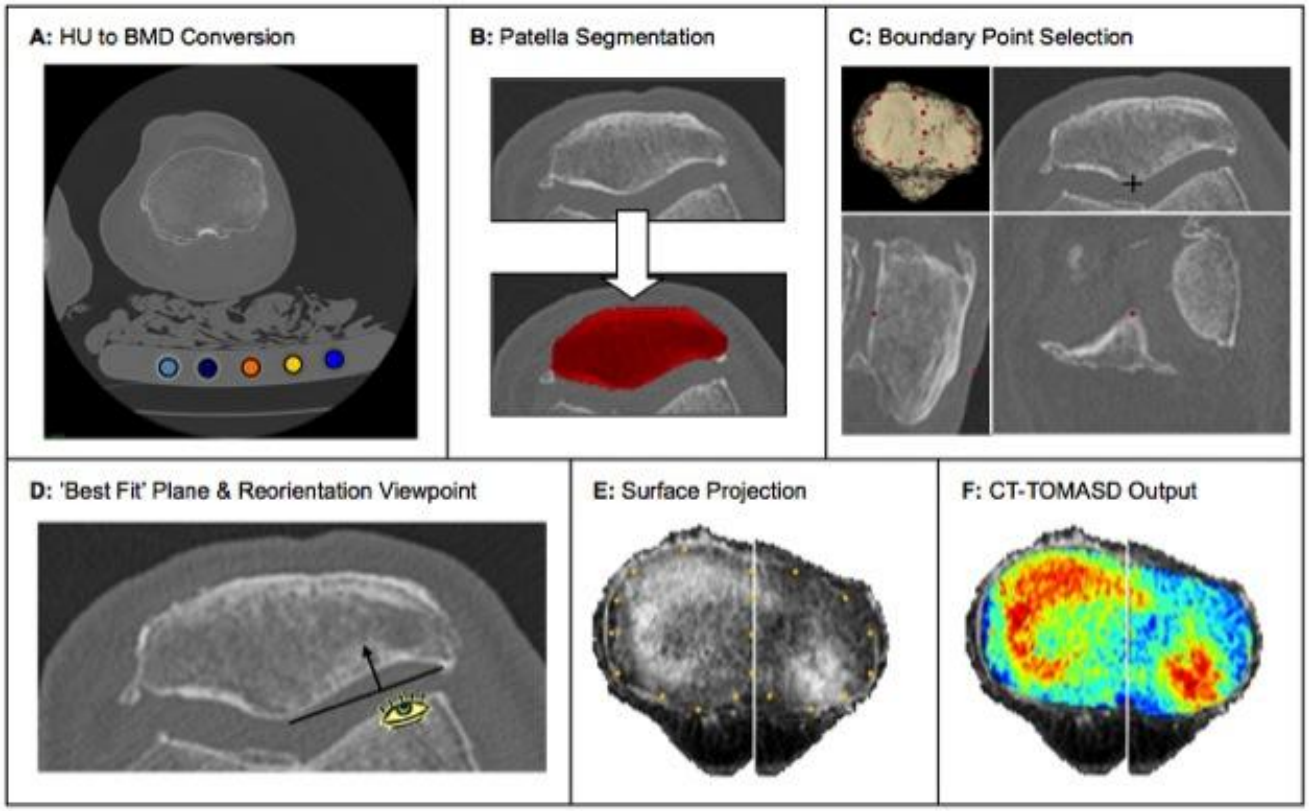

Figure 4-1. Methodological sequence for CT-TOMASD analyses in the patella consists of converting CT grayscale intensity to BMD using a QCT reference phantom (A), followed by semi-automatic patellar segmentation in the transverse plane (B). Peripheral and interior boundary points are manually selected (C) to define medial and lateral facets; with the patella reoriented relative to 'best fit' planes passing through facet boundary points (D). A surface projection image processing algorithm is performed to map 3D subchondral density in relation to depth (measured from the subchondral surface) directly at the patellar surface (E). CT-TOMASD output is represented through colormaps at each successive depth (F).

4.3.3.6. Regional analysis

A series of regional analyses (Figure 4-2) were performed on each 2D projected image (0–2.5mm, 2.5–5mm, and 5–7.5mm layers), including:

1. Lateral and medial BMD
2. Peripheral and central BMD
3. Superior, middle, and inferior compartment BMD, assessed by dividing each facet into three equally spaced subregions [112].

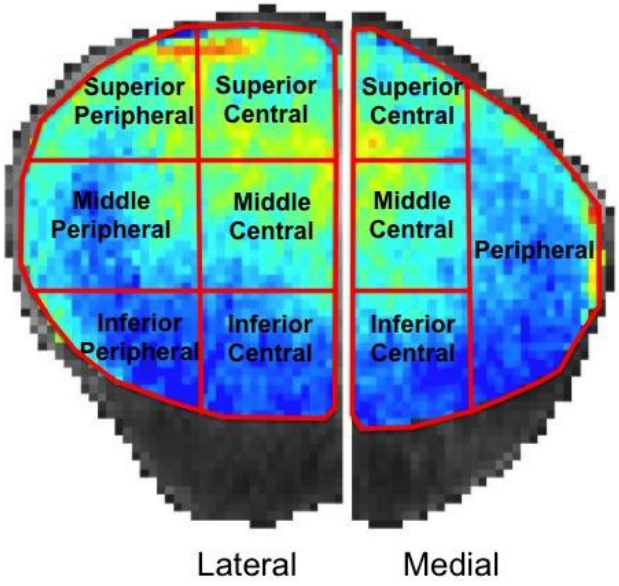

Figure 4-2. Regional analysis on lateral and medial patellar facets consists of superior/middle/inferior as well as central/peripheral divisions.

4.3.4. Statistical Analysis

To assess *in vivo* precision of CT-TOMASD regional density measures, we scanned 14 participants, 3 times each; for a total of 42 scans with 28 degrees of freedom (DOF) [113]. We also assessed the *in vivo* precision of CT-TOMASD regional measurements in OA (7 participants, 21 scans, 14 DOF) and healthy (7 participants, 21 scans, 14 DOF) knees. Precision of each regional analysis is reported using both absolute values (root mean square standard deviation, SD_{RMS}) and as a percentage (root mean square coefficients of variation, $CV\%_{RMS}$) [113]. For comparison with related precision errors, mean BMD values for each regional analysis

are also reported. To assess repeatability of CT-TOMASD measures in the patella, we used a two-way mixed intraclass correlation coefficient (ICC) model [114], which relates inter-subject variance to population variance. Statistical analyses were performed using commercial software (SPSS 20.0, SPSS Inc, Chicago, Il, USA).

4.4. Results

Precision errors associated with CT-TOMASD in the patella were small. $CV\%_{RMS}$ for both OA and healthy participants ranged from 1.1% to 6.8% (average: 2.9%) (Table 4-1). Repeatability was high, with ICC ranging from 0.97 to 1.00. In healthy participants, average $CV\%_{RMS}$ precision errors ranged from 0.7% to 4.9% (average: 2.5%) (Table 4-2), and from 0.9% to 8.6% (average: 3.2%) in participants with OA (Table 4-3). Figure 4-3 shows representative colormaps of a healthy patella (top row) and a patella with OA (bottom row) at three measured depths of 0-2.5mm, 2.5-5mm, and 5-7.5mm. Average precision errors were approximately 4 times smaller than BMD %-difference between OA and healthy patellae.

Table 4-1. Precision results for CT-TOMASD: average BMD measures (mg/cm^3 K_2HPO_4) in healthy and osteoarthritic knees (14 participants, 3 scans each, 28 degrees of freedom). Precision is reported using root mean square standard deviations (SD_{RMS}), coefficients of variation ($CV\%_{RMS}$), and intraclass correlation coefficients (ICC). $CV\%_{RMS}$ also includes range of (minimum to maximum) $CV\%_{RMS}$ values.

Region		Depth											
		0-2.5mm				2.5-5mm				5-7.5mm			
		Mean	SD_{RMS}	$CV\%_{RMS}$	ICC	Mean	SD_{RMS}	$CV\%_{RMS}$	ICC	Mean	SD_{RMS}	$CV\%_{RMS}$	ICC
Lateral facet	Total	592	13.2	1.1 (0.2-2.1)	1.00	376	4.6	1.2 (0.2-2.1)	1.00	354	5.3	1.6 (0.7-2.3)	1.00
	Superior	629	17.6	1.4 (0.2-2.6)	1.00	453	6.1	1.5 (0.2-3.7)	1.00	455	12.4	2.6 (0.3-4.3)	0.99
	Middle	671	6.85	1.1 (0.1-2.6)	1.00	411	10.6	2.5 (0.0-4.8)	1.00	349	10.8	3.2 (0.5-7.2)	0.99
	Inferior	450	23.6	5.7 (0.5-12.8)	0.97	254	8.5	3.8 (0.6-9.0)	0.99	257	7.9	3.1 (0.8-6.7)	0.99
	Superior-Peripheral	693	8.1	1.2 (0.3-2.4)	1.00	502	10.2	1.9 (0.5-3.6)	0.99	559	21.1	3.8 (1.2-6.6)	0.97
	Middle-Peripheral	687	10.6	1.6 (0.4-4.3)	1.00	401	11.9	3.0 (0.8-4.8)	0.99	420	21.1	5.1 (0.1-10.8)	0.98
	Inferior-Peripheral	454	26.6	6.8 (1.2-14.7)	0.97	273	13	5.0 (0.8-12.1)	0.99	354	18.2	5.1 (0.8-7.8)	0.99
	Superior-Central	590	10	1.8 (0.3-3.9)	1.00	425	7.4	1.9 (0.6-4.4)	1.00	390	13.1	2.8 (0.6-7.2)	0.99
	Middle-Central	654	9.7	1.5 (0.2-4.5)	1.00	421	11.3	2.7 (0.8-5.2)	1.00	274	6.5	2.7 (0.5-6.5)	1.00
	Inferior-Central	447	23.8	5.6 (0.7-11.3)	0.97	240	10.2	4.1 (0.6-8.9)	0.99	193	3.5	1.9 (0.2-3.5)	1.00
Medial facet	Total	481	7.3	1.6 (0.7-2.7)	1.00	289	4.7	1.6 (0.5-3.4)	1.00	268	5.8	2.3 (0.7-5.5)	0.99
	Superior-Central	495	13.8	2.6 (0.3-4.8)	0.99	351	6.5	1.8 (0.9-2.7)	1.00	366	16.5	3.7 (0.3-10.7)	0.98
	Middle-Central	568	11.3	2.0 (0.7-4.5)	1.00	331	9.7	2.9 (0.6-5.1)	1.00	250	8.9	3.5 (0.7-6.3)	0.99
	Inferior-Central	443	12.5	4.0 (0.6-11.7)	1.00	223	8.2	4.1 (0.6-9.3)	0.98	185	4.3	2.5 (0.5-5.2)	1.00
	Peripheral	409	15.4	5.0 (0.8-14.5)	0.99	257	7.2	2.8 (0.9-4.1)	1.00	291	12.8	4.4 (1.0-10.4)	0.99

Table 4-2. Precision results for CT-TOMASD: average BMD measures (mg/cm^3 K_2HPO_4) in healthy knees (7 participants, 3 scans each, 14 degrees of freedom). Precision is reported using root mean square standard deviations (SD_{RMS}), coefficients of variation ($CV\%_{RMS}$), and intraclass correlation coefficients (ICC). $CV\%_{RMS}$ also includes range of (minimum to maximum) $CV\%_{RMS}$ values.

Region		Depth											
		0-2.5mm				2.5-5mm				5-7.5mm			
		Mean	SD_{RMS}	$CV\%_{RMS}$	ICC	Mean	SD_{RMS}	$CV\%_{RMS}$	ICC	Mean	SD_{RMS}	$CV\%_{RMS}$	ICC
Lateral facet	Total	615	4.3	0.7 (0.2-0.9)	1.00	407	4.6	1.1 (0.2-1.8)	1.00	382	5.2	1.4 (0.7-2.1)	0.99
	Superior	659	9.3	1.5 (0.2-2.6)	1.00	479	6.7	1.6 (0.2-3.7)	1.00	488	13.1	2.4 (0.3-4.3)	0.99
	Middle	703	7.2	1.1 (0.1-2.2)	1.00	452	11.4	2.3 (0.5-4.0)	0.99	377	7.8	2.1 (0.8-3.2)	0.98
	Inferior	454	15.6	3.6 (0.5-6.5)	0.97	272	7.8	3.0 (0.6-4.5)	0.97	279	8.3	2.8 (0.9-4.6)	0.99
	Superior-Peripheral	712	8	1.2 (0.3-2.3)	1.00	507	7.6	1.4 (0.5-2.2)	1.00	592	15.9	2.7 (1.2-4.1)	0.99
	Middle-Peripheral	711	9.71	1.3 (0.4-2.0)	1.00	427	12.2	2.7 (0.8-4.6)	0.99	434	17.1	3.9 (0.6-6.3)	0.94
	Inferior-Peripheral	447	18.1	4.4 (1.2-7.3)	0.95	289	13.2	4.1 (1.8-6.4)	0.96	384	19.1	4.9 (0.8-6.2)	0.98
	Superior-Central	625	11.3	2.0 (0.3-3.9)	1.00	462	8.6	2.2 (0.7-4.4)	1.00	421	16.6	3.1 (0.6-7.2)	0.99
	Middle-Central	693	12.7	1.9 (0.2-4.5)	0.99	480	13.0	2.6 (0.8-4.8)	1.00	315	7.0	2.1 (1.1-3.4)	0.99
	Inferior-Central	457	17.5	3.7 (0.7-6.7)	0.98	261	11.9	4.3 (0.6-8.9)	0.95	212	4.1	2.1 (0.2-3.5)	0.99
Medial facet	Total	509	7.6	1.5 (0.8-2.3)	0.99	325	5.9	1.8 (0.9-3.4)	0.98	299	5.8	1.9 (0.7-3.2)	0.99
	Superior-Central	511	17.3	3.1 (1.9-4.8)	0.98	384	7.2	1.8 (0.9-2.7)	0.99	402	21.5	4.5 (0.8-10.7)	0.96
	Middle-Central	624	13.6	2.1 (0.7-4.5)	0.98	389	11.3	2.8 (0.6-4.9)	0.99	287	10.1	3.2 (1.3-6.3)	0.97
	Inferior-Central	454	12.5	2.7 (0.6-4.1)	0.99	247	8.9	3.7 (1.7-7.6)	0.99	201	4.5	2.4 (0.5-5.2)	0.96
	Peripheral	441	12.9	2.8 (0.9-5.0)	0.95	287	8.1	2.8 (2.4-3.2)	0.98	331	12.1	3.3 (1.0-7.4)	0.99

Table 4-3. Precision results for CT-TOMASD: average BMD measures (mg/cm^3 K_2HPO_4) in osteoarthritic knees (7 participants, 3 scans each, 14 degrees of freedom). Precision is reported using root mean square standard deviations (SD_{RMS}), coefficients of variation ($CV\%_{RMS}$), and intraclass correlation coefficients (ICC). $CV\%_{RMS}$ also includes range of (minimum to maximum) $CV\%_{RMS}$ values.

Region		Depth											
		0-2.5mm				2.5-5mm				5-7.5mm			
		Mean	SD_{RMS}	$CV\%_{RMS}$	ICC	Mean	SD_{RMS}	$CV\%_{RMS}$	ICC	Mean	SD_{RMS}	$CV\%_{RMS}$	ICC
Lateral facet	Total	569	7.5	1.3 (0.5-2.1)	1.00	345	4.5	1.4 (0.5-2.1)	1.00	326	5.4	1.7 (1.0-2.3)	1.00
	Superior	599	6.8	1.2 (0.3-1.6)	1.00	427	5.5	1.3 (0.5-2.2)	1.00	421	11.7	2.8 (1.3-4.0)	0.99
	Middle	640	6.5	1.2 (0.3-2.6)	1.00	369	9.6	2.8 (0.0-4.8)	1.00	322	13.1	4.0 (0.5-7.2)	0.99
	Inferior	446	29.6	7.3 (0.5-12.8)	0.98	235	9.1	4.5 (1.5-9.1)	0.99	236	7.5	3.3 (0.8-6.7)	0.99
	Superior-Peripheral	675	8.2	1.2 (0.7-2.4)	1.00	497	12.2	2.3 (0.5-3.6)	0.99	525	25.3	4.7 (2.1-6.6)	0.95
	Middle-Peripheral	663	11.5	1.9 (0.5-4.3)	1.00	376	11.5	3.3 (1.1-4.8)	0.99	406	24.4	6.0 (0.1-10.8)	0.99
	Inferior-Peripheral	460	32.9	8.6 (1.6-14.7)	0.98	257	12.7	5.7 (0.8-12.1)	0.99	324	17.3	5.2 (1.4-7.8)	0.99
	Superior-Central	555	8.5	1.6 (1.0-2.5)	1.00	387	6.0	1.5 (0.8-2.4)	1.00	359	8.1	2.5 (1.3-3.9)	1.00
	Middle-Central	616	5.3	0.9 (0.5-1.4)	1.00	361	9.2	2.8 (0.8-5.2)	1.00	234	6.1	3.2 (0.5-6.5)	1.00
	Inferior-Central	436	28.8	6.9 (4.9-11.4)	0.97	219	8.2	3.9 (2.4-5.8)	0.99	175	2.9	1.7 (1.0-2.6)	1.00
Medial facet	Total	452	7.1	1.8 (0.7-2.7)	1.00	253	3.0	1.2 (0.5-1.7)	1.00	238	5.8	2.6 (0.9-5.5)	1.00
	Superior-Central	479	9	1.9 (0.3-2.5)	1.00	319	5.7	1.8 (0.9-2.7)	1.00	330	9.2	2.8 (0.3-4.3)	1.00
	Middle-Central	513	8.5	1.8 (1.2-2.5)	1.00	272	7.7	3.0 (1.1-5.1)	1.00	213	7.6	3.8 (0.7-5.3)	0.99
	Inferior-Central	433	12.5	5.0 (0.7-11.7)	1.00	199	7.4	4.6 (0.6-9.3)	1.00	169	4.0	2.7 (0.3-4.3)	1.00
	Peripheral	378	17.6	6.6 (1.3-14.5)	1.00	227	6.3	2.8 (0.9-4.1)	1.00	250	13.5	5.3 (1.4-10.4)	0.98

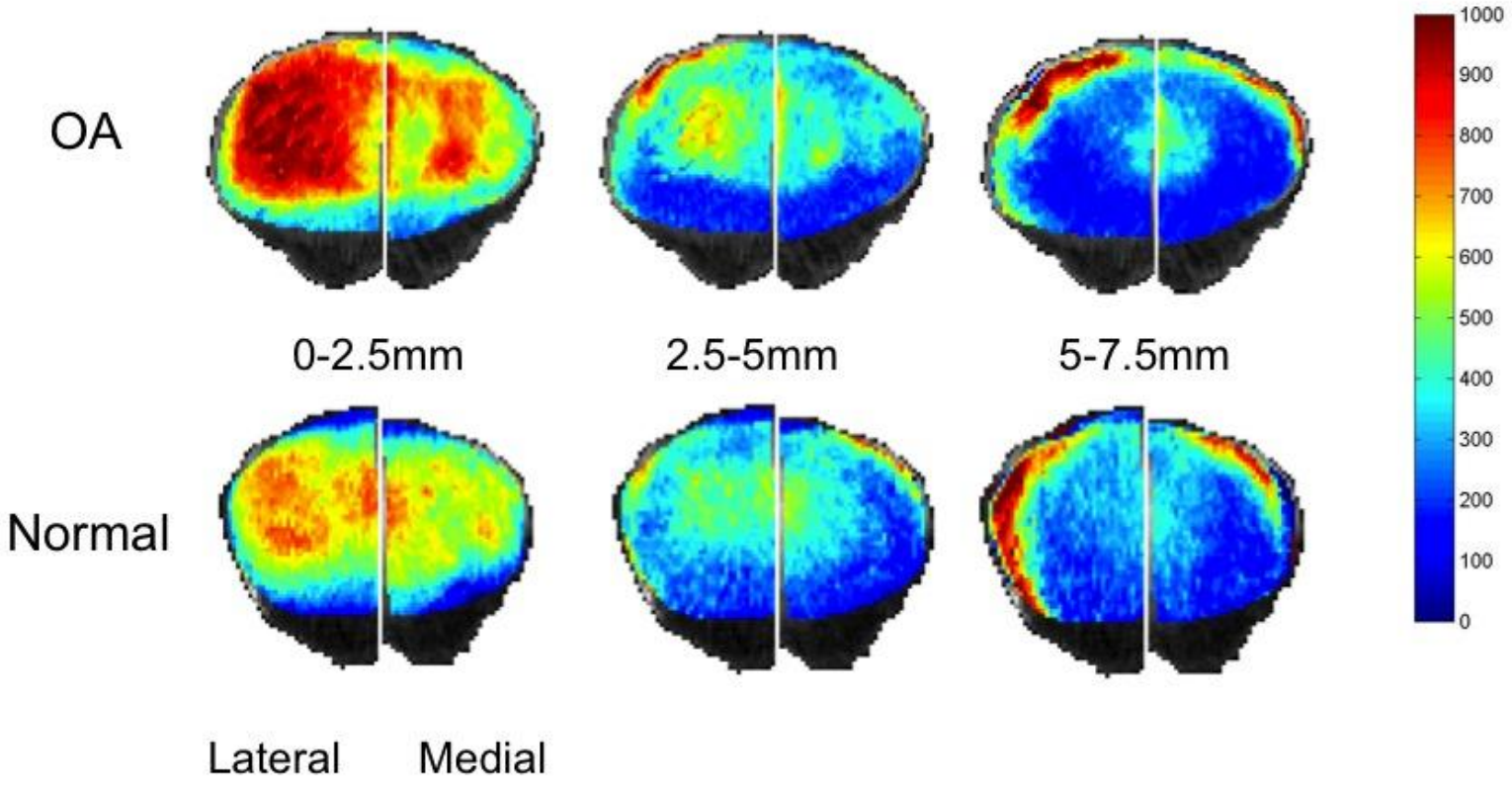

Figure 4-3. Representative topographical color maps of patellar BMD at depths of 0-2.5mm, 2.5-5mm and 5-7.5mm in healthy participants (top row) and participants with OA (bottom row).

4.5. Discussion

We studied the in vivo precision of CT-TOMASD measures of patellar subchondral BMD in knees of healthy individuals and those with OA. This is the first study to report the precision of CT-based BMD values in the patella. This is also the first study to offer *in vivo* measures of subchondral cortical and subchondral trabecular BMD in healthy and OA patellae using clinical QCT.

Our CT-TOMASD measurements show precise (average $CV\%_{RMS}$ less than 5%) *in vivo* measurements of subchondral cortical and subchondral trabecular BMD measured relative to the subchondral surface. These *in vivo* precision errors are within the same range as our preliminary precision results [109] and therefore can be considered trustworthy. Low precision error values are due to the use of small (0.625mm) isotropic voxels and the ability to reliably reconstruct and rotate the 3D image volume in various orientations without compromising resolution in any plane. This characteristic, combined with boundary point selection defining each lateral and medial facet and short scanning time (~90s), allows for the ability to reconstruct the imaged patella in repeatable orientations minimizing the effect of patient positioning.

This study has many strengths: an appropriate number of subjects and scans to establish conservative precision errors, the inclusion of both healthy participants, and a sample with OA, and a comprehensive reporting of precision measures including $CV\%_{RMS}$ and ICC. First, we met conservative recommendations for number of subjects and scans [113], i.e., 28 degrees of freedom with 3 repeated measures on 14 subjects. These recommendations are sufficient to establish reliable precision errors will small confidence intervals (30% higher than mean precision errors) [113]. Second, our study uses images from both healthy and OA knees for precision analysis, offering confident application of the image processing technique to either healthy or OA knees in future studies. The inclusion of both groups in our precision analysis provides representative precision errors for either healthy or OA knees. If precision analysis is limited to only healthy or only OA joints, then results may offer misrepresentative precision errors for comparison between normal and OA subchondral BMD in future studies. Third, we present a comprehensive analysis by including both $CV\%_{RMS}$ and ICC as measures of the reliability of CT-TOMASD in the patella, allowing us to evaluate the reliability of individual density measures. The $CV\%_{RMS}$ measures provide an assessment of the variation in density

measures between multiple scans while the ICC provides a measure of homogeneity, or consistency, of repeated BMD measurements.

Limitations of this study relate to our sample size and OA classification. Although we have met recommendations for conservative determination of precision errors [113] in our overall sample (14 participants, 42 scans, 28 DOF), our mixed sample has participants with OA (7 individuals, 21 scans, 14 DOF) and healthy participants (7 individuals, 21 scans, 14DOF). Our reported $CV\%_{RMS}$ and ICC values represent conservative assessments of CT-TOMASD precision in a range of participants with and without OA. This was deliberate as we wanted to increase the variability of BMD measures in our precision measurement for use of CT-TOMASD in future studies comparing participants with and without OA. Independently determining precision errors for samples with and without OA would require twice as many participants (14 with OA and 14 without OA) and would inflict unnecessary radiation to more participants. Our separate analysis of participants with OA and participants without OA yielded similar precision errors as the combined sample, so our decision to combine groups to meet conservative recommendations [113] is justified. Secondly, our OA classification was performed retrospectively through CT volume reconstruction as opposed to being based on a clinical diagnosis. Clinical OA classification is performed by assigning KL grade qualifiers [58] to individual joints and requires a series of radiographs in various orientations; and would increase effective radiation dosage in participating volunteers.

There are also certain limitations with the CT-TOMASD image processing tool that need to be considered. The 2D projection nature of CT-TOMASD could induce over- or under-estimation of density at the subchondral bone surface in regions with excessive curvature [23], particularly around the patellar periphery. To reduce these effects, we used best-fit planes and reorientations, then reconstructed each volume to find the position with the lowest curvature on each facet. Also, we used an image-specific HMH threshold [110] to locate the subchondral surface of each unique patellar volume, as well layer analyses averaging density over different depths of 2.5mm from the surface. The combination of techniques minimizes the effect of partial volume artifacts at the subchondral surface. Another limitation of the CT-TOMASD technique is the amount of manual, and possibly subjective, intervention. Even though patient-specific boundary points are selected while referring to all three orientations (transverse, coronal, and

sagittal) to ensure correct placement, they are manually selected possibly increasing user-induced error.

On the anterior patellar surface, our precision errors were largest in peripheral regions where the effect of partial volume artifacts could be high. However, the precision errors of superior/middle/inferior regions are generally low (<5%), with peripheral regions having little effect on total region precision. For these reasons, we believe that the effects of the anterior patellar surface on CT-TOMASD measures are small. Second, as with any QCT-based imaging technique, participants are exposed to ionizing radiation. As the knee has a low presence of radiosensitive tissues, QCT analyses at this location result in a low effective dosage (~0.073mSv) [23].

4.6. Conclusion

Regional patellar *in vivo* CT-TOMASD precision errors ranged from 1.1% to 6.8% at depths of 0-2.5mm, 1.2% to 5.0% at depths of 2.5-5mm and 1.6% to 5.1% at depths of 5-7.5mm in a sample of healthy and OA participants. These results suggest that this technique has the potential to identify and quantify OA-associated subchondral BMD changes in the patella, *in vivo*.

CHAPTER 5
CT-TOMASD IN PATIENTS WITH CLINICALLY DIAGNOSED OA

5.1. Synopsis

This chapter describes our study using CT-TOMASD to measure BMD at three successive depths (0-2.5mm, 2.5-5mm and 5-7.5mm) in a group of participants with clinically diagnosed OA. The participants were divided into two groups—those experiencing 'severe pain at rest' and those experiencing 'non-severe pain at rest'. Participants experiencing 'severe pain at rest' had lower BMD at depths consisting primarily of trabecular bone than participants experiencing 'non-severe pain at rest'.

5.2. Introduction

Although generally considered a disease related to cartilage, OA is marked by changes to many joint tissues [9, 54, 115], including the underlying subchondral bone [116]. Cartilage is aneural and insensate [22], but underlying subchondral bone is innervated [19, 117] and could be a factor in OA-related pain. Trabecular bone has a greater concentration of nerve endings than cortical bone [75] and could be an initiation site for pain.

OA-related pain at rest (e.g., sitting, lying down, nocturnal pain) is of great concern to patients because it is related to sleeplessness and other disruptions in quality of life [62]. Although pain is related to clinical radiological measures of PF OA disease severity (e.g., sclerosis, osteophyte presence) [12, 66, 67], the strongest relationships are present in cases with severe OA [11]. This could be due to the inherent limitations of 2D imaging modalities, including limited radiographic skyline views of the patella and projection images (which may superimpose radiographic features of OA). Currently available 3D imaging modalities, such as QCT, allow the patella to be viewed from all angles and can also be used to assess 3D subchondral BMD [103]. CT-TOMASD has the potential to determine BMD measurements at progressive depths that approximate distinctions between subchondral cortical BMD and trabecular BMD layers [23], which may have different roles linked to OA-related pain.

The objective of this study was to determine whether there are measurable differences in patellar subchondral BMD between OA patients with different pain experiences, particularly pain at rest.

5.3. Methods

5.3.1. Study Sample

Fifty-two participants (23M:29F; mean age 64, SD±9years) were recruited for this study prior to total knee replacement. Study exclusion criteria included pregnant women, participants having a revision knee replacement instead of primary knee replacement, prior history of bone pathology at the knee joint, and those who were not able to complete the OA severity index tests. We excluded any images with excessive imaging artifacts, motion artifacts or incomplete images, leaving 42 participants (17M:25F; mean age 64, SD±10years).

5.3.2. Clinical Assessment

Each participant was assessed for pain at the affected knee joint using a 5-point Likert scale of the pain subsection of the Western Ontario McMasters Osteoarthritis Index (WOMAC) [8, 118], which evaluates 5 pain items, 17 function items and 2 stiffness items. Participants were asked to assess the level of pain in the affected knee joint within the past 24-hours while walking on a flat surface, going up or down stairs, lying in bed, sitting or standing upright.

We defined ‘at rest’ by dividing the WOMAC pain subsections into rest activities (lying in bed, sitting down) and weight-bearing activities (walking, up/down stairs) [64, 78] and considered any participants who scored a 3 (severe pain) or 4 (extreme pain) in either rest activity (while lying down or sitting) as having ‘severe pain at rest’. Those not scoring a 3 or 4 in either rest activity were considered to have ‘non-severe pain at rest’ [119]. No patients scored 0 (no pain) in both rest activities. The sample was divided with 21 participants in the ‘severe pain at rest’ grouping and 21 participants in the ‘non-severe pain at rest’ grouping (Table 5-1). All patients had radiographic OA severity of KL grade 3 or 4.

Table 5-1. Background characteristics and clinical data for 'non-severe pain at rest' and 'severe pain at rest' groups. There were no differences between groups in age and BMI (assessed using t-tests) or sex (assessed using χ^2 test).

	Non-severe Pain at Rest (N=21)	**Severe Pain at Rest (N=21)**
WOMAC	0, 1 or 2	3 or 4
Sex Ratio	9M:12F	8M:13F
Age in years (mean ± SD)	65.0 ± 10.4	63.2 ± 9.93
BMI in kg/m^2 (mean ± SD)	29.1 ± 3.05	28.2 ± 4.23
KL Grade	3 to 4	3 to 4

5.3.3. CT Acquisition

We collected CT data using single-energy quantitative CT (QCT) via a clinical CT scanner (Lightspeed 4-slice, General Electric, Milwaukee, WI, USA). Participants were oriented supine within the CT gantry, with both legs scanned simultaneously. Below the patients' legs, we included a solid QCT reference phantom (Model 3T, Mindways Software Inc, Austin, TX, USA) to convert grayscale CT Hounsfield Units (HU) to equivalent apparent BMD (mg/cm^3 K_2HPO_4). Scans of both knees included the distal femur, the proximal tibia and the patella; though only the patella was used in this analysis. CT scanning parameters included: 120kVp tube voltage, 150mA tube current, axial scanning plane, 0.625mm isotropic voxel size (0.625mm slice thickness, 0.625 x 0.625mm in-plane pixel size), ~254 slices, ~60s scan time and 0.073mSv radiation dosage. A standard bone kernel (BONE) was used for CT image post-processing.

5.3.4. CT Image Analysis

The imaging methodology used has been previously described in detail (Chapter 4). We followed the same process for BMD conversion, segmentation, alignment, surface projection, and normalization. The regional analysis was modified as we only focused on the superior, middle, and inferior regions of the lateral facet.

5.3.5. Regional analysis

We performed a regional analysis of the lateral facet on each 2D projection image (0-2.5mm, 2.5-5mm and 5-7.5mm layers); dividing the surface of the lateral facet into three equally spaced sections relative to superior-inferior height (Figure 5-1). We report average BMD on the following surfaces: total lateral facet, superior lateral facet, middle lateral facet, and inferior lateral facet; as the lateral facet has up to 60% more load applied than the medial facet [30]. We defined depths between 0-2.5mm as the patellar subchondral cortical region based on reported cortical thickness of 0.1-2.1mm [120] and depths beneath 2.5mm as trabecular bone regions based on average BMD below 400mg/cm^3 [35].

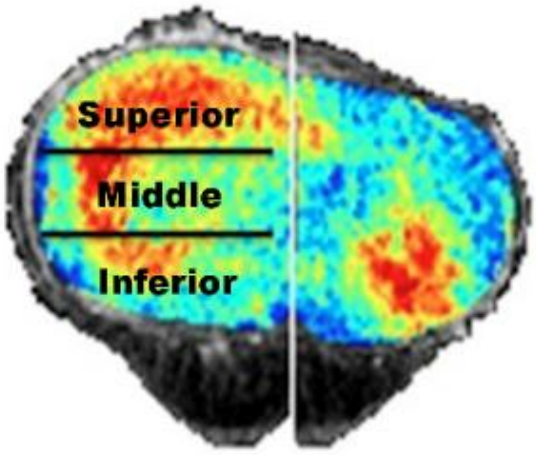

Figure 5-1. Position of superior, middle and inferior regions on lateral patellar facet.

5.3.6. Statistical Analysis

We first tested the equality of variances in subchondral BMD outcomes using Levene's test and between group differences in potential confounding factors for BMD with χ^2 test (sex) and t-tests (age, body mass index (BMI)). There were no differences in BMD variances or sex distribution, age, and BMI between the 'severe pain at rest' and 'non-severe pain at rest' groups (Table 5-1), therefore we used independent t-tests to compare between group differences in mean subchondral patellar BMD across regions. We report mean and standard deviation (SD) for lateral surface BMD outcomes for both groups, as well as mean %-differences with 95% confidence intervals for pair-wise comparisons between 'severe pain at rest' and 'non-severe

pain at rest' groups. We considered an α-level less than 5% statistically significant. Statistical analyses were performed using commercial software (SPSS 19, SPSS Inc, Chicago, IL, USA).

5.4. Results

Across the total lateral facet, there was a trend towards lower total BMD at each successive depth in participants experiencing 'severe pain at rest' compared to those with 'non-severe pain at rest' (Figure 5-2). Mean BMD was 16.7% lower at the 5-7.5mm depth in the total lateral facet in patients with 'severe pain at rest' (mean difference: - 53mg/cm^3; 95% CI: -103 to -3mg/cm^3; p=0.04) (Table 5-2, Figure 5-2, Figure 5-3, Figure 5-4).

Regionally, mean BMD was 16.4% lower at the 5-7.5mm depth in the superior lateral facet in patients with 'severe pain at rest' (mean difference: -67mg/cm^3; 95% CI: -131 to -4mg/cm^3; p=0.04) (Table 5-2, Figure 5-2, Figure 5-3, Figure 5-4). BMD was also lower in the lateral inferior region in the 'severe pain at rest' group at each depth from the subchondral bone surface (Figure 5-2). BMD at the inferior lateral facet was 13.1% lower at the 0-2.5mm depth (mean difference: -66mg/cm^3; 95% CI: -125 to -7mg/cm^3; p=0.03), 23.0% lower at the 2.5-5mm depth (mean difference: -62mg/cm^3; 95% CI: -104 to -20mg/cm^3; p=0.005), and 21.8% lower at the 5-7.5mm depth (mean difference: -52mg/cm^3; 95% CI: -95 to -9mg/cm^3; p=0.02) (Table 5-2, Figure 5-2, Figure 5-3, Figure 5-4). There were no observed differences at other regions or depths.

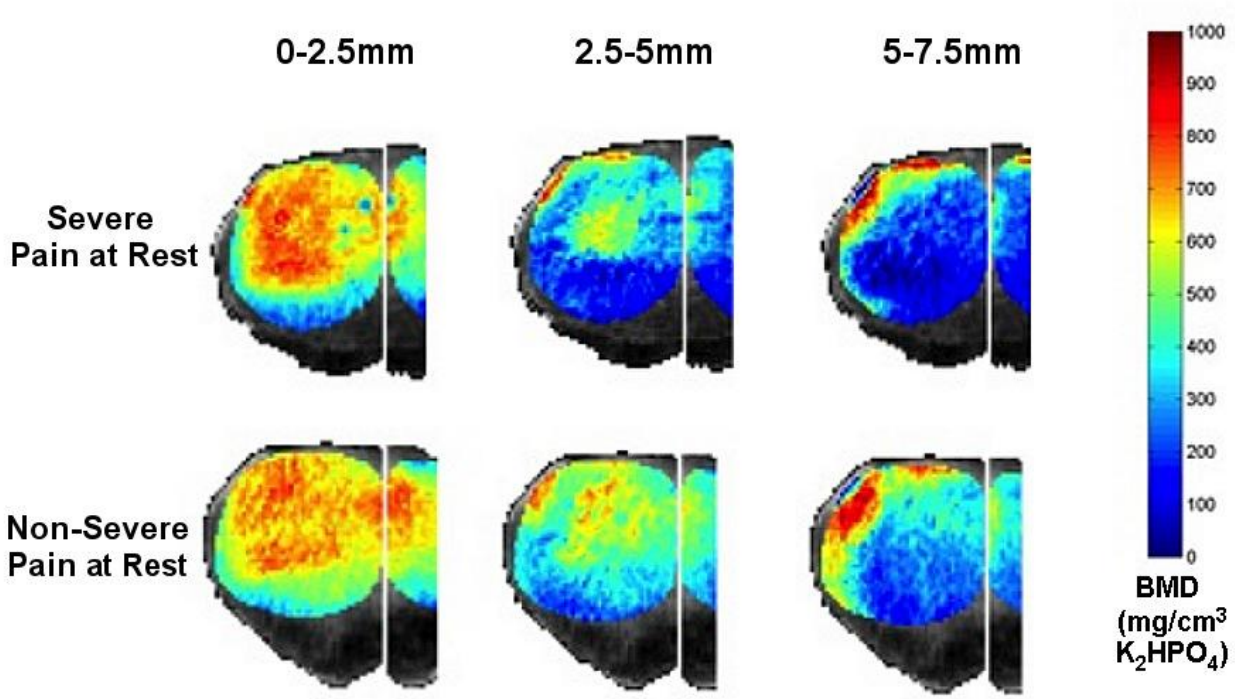

Figure 5-2. Representative topographical color maps of average lateral patellar BMD at depths of 0-2.5mm, 2.5-5mm and 5-7.5mm in participants reporting ‘severe pain at rest’ (top row) and ‘non-severe pain at rest’ (bottom row).

Table 5-2. Mean ± standard deviation (SD), absolute mean difference, percent difference, 95% confidence intervals (CI) and *p*-value of bone mineral density (BMD) measurements in patients with knee osteoarthritis with 'severe pain at rest' and 'non-severe pain at rest'.

Region	Depth	BMD (mg/cm^3 K_2HPO_4)		Mean difference (%)	95% Confidence Interval (mg/cm^3 K_2HPO_4)		P-value
		Severe Pain	Non-severe Pain				
		Mean ± SD	Mean ± SD		Lower Limit	Upper Limit	
Lateral Facet							
Total	0-2.5 mm	522 ± 82	557 ± 94	-35 (-6.3%)	-90	20	0.21
	2.5-5 mm	298 ± 87	347 ± 82	-49 (-14.1%)	-101	4	0.07
	5-7.5 mm	263 ± 77	316 ± 84	-53 (16.7%)	-103	-3	0.04
Superior	0-2.5 mm	554 ± 88	573 ± 104	-19 (-3.3%)	-80	40	0.51
	2.5-5 mm	353 ± 95	405 ± 106	-52 (-12.8%)	-115	11	0.10
	5-7.5 mm	341 ± 94	408 ± 110	-67 (-16.4%)	-131	-4	0.04
Middle	0-2.5 mm	559 ± 93	586 ± 104	-27 (-4.6%)	-88	35	0.39
	2.5-5 mm	323 ± 104	366 ± 98	-43 (-11.7%)	-106	20	0.17
	5-7.5 mm	262 ± 90	312 ± 97	-50 (-16.0%)	-109	7	0.09
Inferior	0-2.5 mm	438 ± 94	504 ± 94	-66 (-13.1%)	-125	-7	0.03
	2.5-5 mm	208 ± 75	270 ± 59	-62 (-23.0%)	-104	-20	0.005
	5-7.5 mm	187 ± 71	239 ± 66	-52 (-21.8%)	-95	-9	0.02

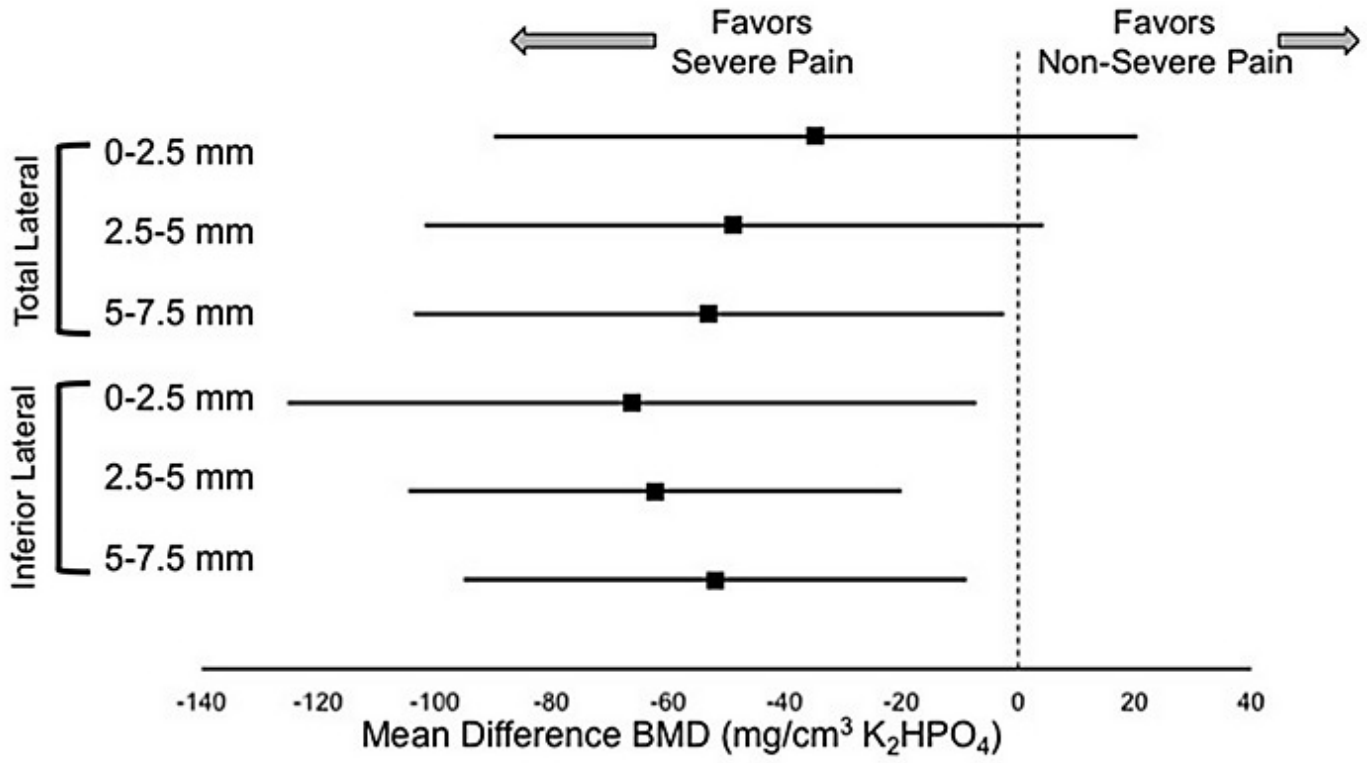

Figure 5-3. 95% confidence intervals (CI) of mean difference in BMD between 'severe pain at rest' and 'non-severe pain at rest' groups in the total lateral facet (top 3 intervals) and inferior lateral facet (bottom 3 intervals) at depths of 0-2.5mm, 2.5-5mm and 5-7.5mm.

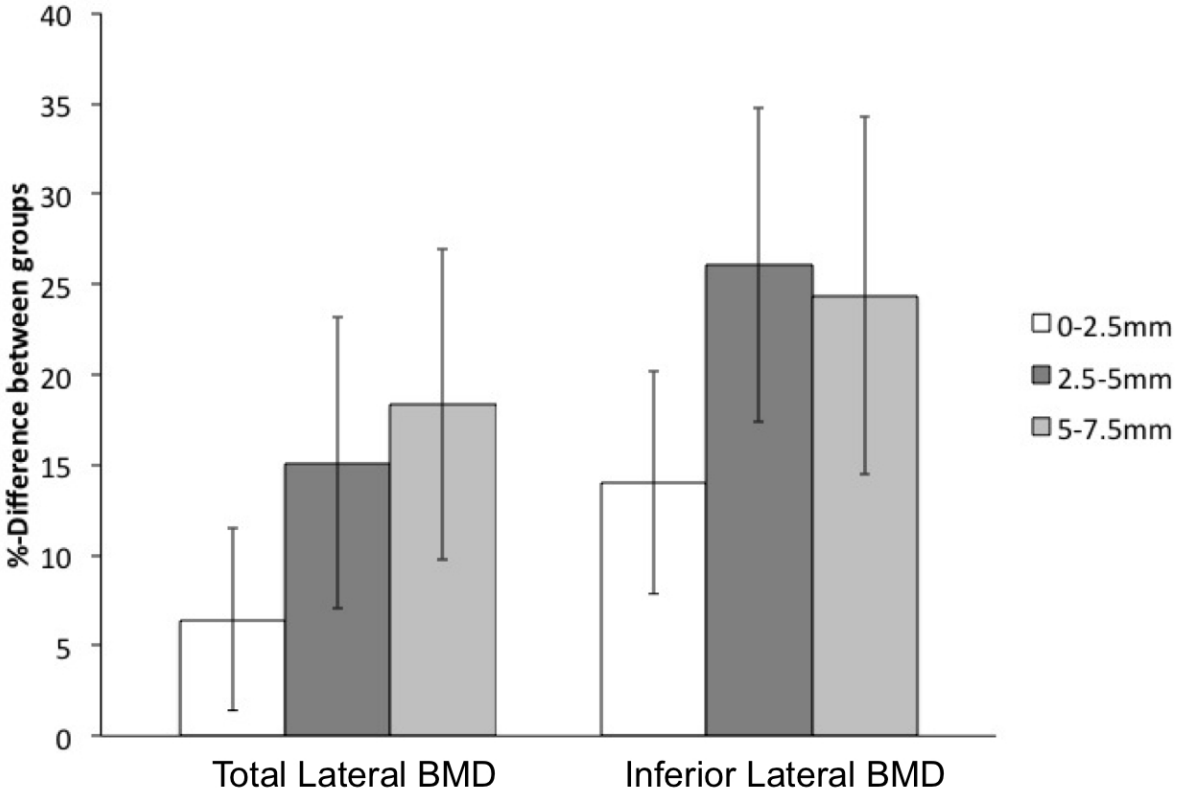

Figure 5-4. Percentage difference in total lateral BMD (left) and inferior lateral BMD (right) between patients showing ‘severe pain at rest’ and ‘non-severe pain at rest’. Error bars represent percentage standard error of difference.

5.5. Discussion

The CT-TOMASD method detected lower patella BMD across various depths and regions in OA patients with ‘severe pain at rest’ when compared to OA patients with ‘non-severe pain at rest’. This is the first study to assess depth-specific bone density in the patellar subchondral region. This is also the first study to link local patellar bone density with pain. These findings suggest that there may be previously unobserved changes in patellar subchondral bone density relating to OA, particularly in patients experiencing ‘severe pain at rest’.

The CT-TOMASD image processing technique demonstrated lower patellar BMD in the ‘severe pain at rest’ group when compared alongside the ‘non-severe pain at rest’ group, with large differences observed at depths of 2.5-5mm (p=0.005) and 5-7.5mm (p=0.02) (which consist primarily of trabecular bone). Our results suggest that low subchondral trabecular bone density may have a role in OA-related pain pathogenesis.

Our findings are consistent with prior research reporting OA-related alterations in subchondral trabecular bone. A pQCT study of the patella [96] has reported decreased trabecular BMD with progressing OA severity. Canine studies have reported lower trabecular BMD in posttraumatic OA-affected joints than in healthy joints [121, 122]. Our results suggest that subchondral trabecular bone may be a key area of interest in the OA knee.

Our study has revealed a potential area where current tools and OA-assessment techniques may be limiting. Reported correlations between radiographic measures of OA (e.g. osteophyte presence, sclerosis) and pain are poor but significant in cases where pain is severe-to-extreme (WOMAC) and OA severity is high (KL) [11, 53, 123]. The KL scale [58] combines osteophyte presence, joint space narrowing and sclerosis (which is essentially high BMD) to determine disease severity in standardized skyline [74] views to assess OA severity in the patella. Although the KL technique may be sufficient in a clinical setting, poor relationships between disease severity and pain could be due to two separate complications. First, disease severity is partly based on the measurement of sclerosis. In this study, we found that lower localized BMD—as opposed to sclerotic bone with high BMD—is significantly related to pain, providing evidence for a new potential area of interest in the investigation of the role of bone in OA. Second, the use of 2D radiographs does not allow the patella to be viewed from all angles, potentially allowing other features in other regions not seen in skyline view, like the inferior lateral facet, to be overlooked. This emphasizes the need to use other imaging modalities such as

3D QCT and image processing tools such as CT-TOMASD when assessing the relationship between pain and subchondral bone changes.

This study has specific strengths. First, this was a homogeneous sample of OA patients scheduled for knee arthroplasty with similar distribution of possible confounding factors (age, sex, BMI) for BMD in both 'severe pain at rest' and 'non-severe pain at rest' groups. We were therefore able to focus our analysis on comparing BMD measurements without adjusting for possible confounding factors. Second, using 3D QCT and CT-TOMASD we measured the density of thin subchondral bone layers near the patellar subchondral bone surface. Such measures would be fundamentally unreliable had they been acquired using 2D imaging tools such as clinical radiography or dual energy x-ray absorptiometry (DXA). Other 3D imaging tools are unable to perform density measurements of subchondral bone layers near the articulating surface. Third, we aligned all patellae in similar 3D orientations relative to landmark boundary points and best-fit planes. This minimized BMD differences due to dissimilar orientations, thereby permitting reliable comparisons between groups.

This study has certain limitations that require consideration regarding pain location and participant physical activity. First, clinical pain assessment for the participants was based upon the entire knee, including the patella, proximal tibia, distal femur, tibiofemoral joint and patellofemoral joint. For this reason, we are uncertain if pain at rest originated from the patella, other tissue, or a combination of tissues. Second, patient physical activity level was unknown—which could affect BMD measurements[124]—and we are uncertain if the observed lower BMD in the 'severe pain-at-rest' group was a result of inactivity, as a result of pain. To address this concern we estimated bone strength by measuring and comparing cortical cross-sectional area at the 66% site proximal to the distal tibial end-plate[125] using independent t-tests (data not shown); and found no difference between 'severe pain at rest' and 'non-severe pain at rest' groups (p=0.61), implying that both groups had similar levels of bone strength, thus similar physical activity levels [126].

Although speculative, it is worthwhile hypothesizing why a loss of trabecular bone may be related to pain at rest. Our preliminary finite element (FE) analyses of articulating bones, though limited to the proximal tibia [127], have shown that trabecular bone (as opposed to commonly assumed subchondral cortical bone) has the most dominant effect on overall structural stiffness at bony ends. Using these FE findings as a guide, a loss of trabecular bone in the patella

will lead to a more flexible structure. Pain may then arise from increased strain or deformation (due to increased flexibility) of remaining trabeculae supporting overlying subchondral cortical bone and cartilage. Increased trabecular strain may also increase strain in subchondral cortical bone (due to increased bending) leading to pain. Various researchers have also theorized links between pain and intraosseous pressure [6, 83]. In line with this theory, local trabecular bone loss may alter intraosseous pressure distributions, leading to increased local pressure and pain. Further research is needed investigating potential links between bone mechanics and pain.

5.6. Conclusion

This study found that total and superior lateral facet BMD was lower in patients experiencing ‘severe pain at rest’ than patients with ‘non-severe pain at rest’ across the 5-7.5mm depth. BMD at the inferior lateral facet was lower in participants with ‘severe pain at rest’ at each depth, particularly in regions comprised of trabecular bone. This study suggests that subchondral trabecular bone may be involved in OA-related pain.

CHAPTER 6
INTEGRATED DISCUSSION

6.1. Overview of findings

CT-TOMASD is a QCT-based imaging program able to perform regional analyses near the articulating surface of the patella in both cortical (0-2.5mm) and trabecular (2.5-5mm and 5-7.5mm) bone layers. It overcomes various limitations of other bone imaging modalities, e.g., radiographs and DXA are limited to 2D imaging and are unable to distinguish between trabecular and cortical bone; MRI does not depict bone mineralization is best suited for measuring trabecular bone, rather than cortical bone; and pQCT is limited to a single axial image. CT-TOMASD is capable of overcoming all these limitations by using a 3D imaged volume to measure regional BMD at various depths from the subchondral surface. As demonstrated in this study, CT-TOMASD could be used to precisely measure *in vivo* patellar subchondral BMD in patients with clinically diagnosed OA, which could help clarify the role of subchondral bone changes in OA progression and potentially providing vital information in improving OA diagnosis and treatment.

A key accomplishment of **Chapter 4 – *In* vivo Precision of CT-TOMASD Measures at the Patella** is that we demonstrated CT-TOMASD could be used to measure, *in vivo,* patellar subchondral BMD in OA and normal knees with precision errors many times smaller than differences between OA and normal density (~4x smaller on average). We found that CT-TOMASD was capable of precisely imaging distinct subchondral bone layers with low precision errors (mean $CV\%_{RMS}$ <5%). The *in vivo* precision errors reported in this study represent a worst-case scenario, as they include the possibility of patient positioning and movement errors with a widely available commercial CT system in a routine environment. This is important because we can now confidently use CT-TOMASD to assess BMD differences between OA and healthy patellae from a clinical setting. Our results show that CT-TOMASD is a versatile technique that can be confidently applied to the articulating patellar surface, as well as the previously explored tibia [23, 24, 26].

The first key accomplishment of **Chapter 5 –CT-TOMASD in Patients with Clinically Diagnosed OA** is that we presented, for the first time, 3D patellar subchondral cortical and trabecular BMD values from a clinical sample of OA patients experiencing knee pain. As a second key accomplishment, we found that patients with ‘severe pain at rest’ had lower BMD in

the inferior regions of the patella than individuals with 'non-severe pain at rest', particularly at depths where trabecular bone was prominent (2.5-5mm and 5-7.5mm). This study shows that subchondral cortical and subchondral trabecular bone may play different roles in OA-related pain, and trabecular bone may be a key site of interest in relation to pain pathogenesis.

6.2. Comparison to Existing Findings

Our *in vivo* precision of CT-TOMASD in the patella is similar to previously reported *in vivo* precision in the tibia [26], as well as a pilot precision study in the patella [109]. CT-TOMASD precision errors ($CV\%_{RMS}$) in the patella range from 1.1% to 6.8% in the 0-2.5mm layer, from 1.2% to 5.0% in the 2.5-5mm layer, and from 1.6% to 5.1% in the 5-7.5mm layer. CT-TOMASD precision errors ($CV\%_{RMS}$) in the tibia ranged from 0.9% to 3.9% in the 0-2.5mm layer, from 1.6% to 4.0% in the 2.5-5mm layer, and from 1.5% to 3.0% in the 5-10mm layer [26]. Our ICCs for CT-TOMASD measures in the patella ranged from 0.95 to 1.00, similar to previously reported ICC values in the tibia [23]. Previous studies using DXA to measure patellar aBMD showed similar $CV\%_{RMS}$ of 1.0%, with an ICC of 0.995 [100], showing that CT-TOMASD in the patella is just as precise as the current standard BMD measurement tool.

Comparisons between CT-TOMASD BMD measures in the patella and existing findings are difficult given that this study presents the only reported subchondral cortical BMD measures in normal and OA patellae. Our BMD values of patellar subchondral trabecular BMD (at depths of 2.5-5mm and 5-7.5mm) are comparable with existing pQCT measures in patients with and without OA [96] (Table 2-5). Reported values of 410 mg/cm^3 in healthy individuals and 340mg/cm^3 in individuals with advanced OA [96] are similar to our measurements at depths of 2.5-5mm (mean BMD of 378 mg/cm^3 in healthy individuals, mean BMD of 316 mg/cm^3 in individuals with OA) and 5-7.5mm (mean BMD of 360 mg/cm^3 in healthy individuals, mean BMD of 301 mg/cm^3 in individuals with OA); showing that our results are similar to other patellar BMD measurements.

In the case of a comparison to symptomatic measures, this is the first study to compare BMD and OA-related pain using WOMAC. DXA studies exploring the relationship between PF pain and aBMD report lower aBMD in the affected knee [99, 100, 102] as well as increased bone turnover in patellae affected with PF pain syndrome [69]. The fundamental limitation of DXA is that the ROI includes the entire patella; it is not possible to isolate specific regions or tissues

within the DXA projection image. Our results also parallel previous studies examining patellar BMD and pain [99, 100, 102], but we were able to isolate the region (inferior lateral facet) and bone tissue layer (trabecular bone) associated with lower BMD using CT-TOMASD. This study identified that trabecular bone may specifically connected to pain.

6.3. Study Strengths

This thesis research has various strengths related to the CT-TOMASD technique and clinical applications of CT, which require further explanation or have not yet been discussed.

CT-TOMASD uses various techniques that allow for analysis of reasonably flat articulating surfaces, such as the patella. First, our clinical CT images were collected using very small isotropic voxels (0.625mm x 0.625mm x 0.625mm). This allows multi-planar data reformations in multiple orientations. This is important, as previously discussed in the tibia [23, 26], but it even more so in the patella, as it appears as a free-floating bone within the complete CT image stack. Using isotropic voxels and 3D image reconstruction allows the entire patellar volume to be isolated for analysis independent of joint positioning or alignment. Patellar alignment can differ between patients, possibly complicating positioning for typical 2D projection analysis through DXA. Small voxel size allows measuring and monitoring small changes, and is especially important in the patella because it's a relatively small bone compared to the other bones in the knee joint. Small voxel size also permits measurement of thin layers, again especially important in the patella because the subchondral cortical layer may range from 0.1mm to 2.09mm [120].

This research presents the possibility of assessing BMD as a clinical measure of OA. Our results show that clinical CT has capabilities to show previously unmonitored differences in trabecular BMD between patients with differing pain experiences. Interestingly, we found lower BMD—a characteristic currently overlooked when determining OA severity. Radiographs subjectively measure sclerosis, or regionally high BMD, which may measure the wrong phenomenon; potentially having overlooking certain cases of OA. This phenomenon may also partially explain why some patients are reporting joint pain, without showing radiographic evidence of OA. Loss of bone density, as opposed to increased bone density, may thus play a role in OA initiation and pain pathogenesis.

6.4. Study Limitations

This thesis research has various limitations related to the study design, study sample size, and associated limitations of CT-TOMASD.

First, our study design lacked a control sample of healthy subjects representing normal patellar BMD values. Our 'severe pain at rest' and 'non-severe pain at rest' groups were naturally formed groups within out subject sample representing a convenient subject variable as opposed to a more powerful independent variable. Ideally, for a stronger analysis, a healthy sample should be used to compare OA BMD with normal BMD to determine if there is a causal relationship between BMD and pain. In our precision analysis, there is a small sample of normal joints (n=7), showing trends of higher patellar BMD in healthy joints, but the sample is too small to perform powered statistical analysis.

Second, our clinical sample size was relatively small. Although 42 subjects, 21 in each group, was large enough to provide significant differences and is of similar group size with previous studies [33, 96, 97], it is too small to determine if changes in BMD were related to other confounding factors such as sex or BMI. However, as some of the observed differences were significant, sample sizes from this study could be used in power analysis for future work.

Third, a limitation of the CT-TOMASD technique is that the process is rather time-consuming as each individual analysis takes about 20 to 25 minutes, with approximately 80% of the analysis time in the segmenting portion. Although the process in the patella is less time consuming than previously reported in the tibia [23], it is still the rate limiting step. Automating segmenting would accelerate the analysis, and may also reduce precision errors. There is a small amount of manual editing during the segmenting process, in most cases close to the peripheral subchondral surface. Boundary point selection is also a manual process; although it is not time consuming, it does require a subjective user decision. Eliminating these manual portions could improve or prevent subjective user decision-making, improving reproducibility [128].

6.5. Conclusions

1. CT-TOMASD can be confidently applied to the patella to measure subchondral cortical and trabecular bone density, with similar level of precision as previously reported at the tibia. Regional patellar CT-TOMASD precision errors ranged from 1.1% to 6.8% at depths

of 0-2.5mm, 1.2% to 5.0% at depths of 2.5-5mm and 1.6% to 5.1% at depths of 5-7.5mm in a sample of healthy and OA participants. Precision errors were many times smaller than observed density differences between patients with differing pain experiences (~4x smaller).

2. Patellar subchondral BMD was lower in patients experiencing 'severe pain at rest' in total lateral facet, particularly in the inferior lateral facet.
    a. Over the total lateral facet, patients experiencing 'severe pain at rest' had 17% lower BMD at depth of 5-7.5mm than patients experiencing 'non-severe pain at rest'.
    b. Regionally, at the inferior lateral facet, patients experiencing 'severe pain at rest' showed 13%, 23%, and 22% lower BMD at depths of 0-2.5mm, 2.5-5mm, and 5-7.5mm depth respectively.

6.6. Contributions

This thesis research has generated many 'firsts' (listed below) and has potential to change clinical BMD measurement from widely used 2D techniques (i.e., DXA) to 3D techniques (i.e., QCT).

1. First study to simultaneously measure patellar subchondral cortical and trabecular BMD using clinical QCT.
2. First application of CT-TOMASD technique to a sample of knees with clinically diagnosed OA.
3. First reporting of relationships between regional localized patellar BMD and pain, specifically pain at rest, showing that individuals with 'severe pain at rest' have lower BMD in deeper trabecular layers than individuals with 'non-severe pain at rest'.

6.7. Clinical significance

Current OA clinical measurement systems, such as the KL grade, use radiographic elements such as sclerosis, or regionally high BMD, to measure OA severity. In our clinical study we found that patients with more pain at rest actually had lower BMD—a measure not currently used to classify OA severity, or even detect presence of OA. This study suggests a previously unexplored clinical measure potentially linked to pain and OA severity.

Current diagnostic tools are limited in detecting OA progression for optimal patient management. This could be due to limitations in current imaging tools or due to symptomatic presentation. CT-TOMASD is a clinical QCT-based tool having the potential to monitor small, localized BMD changes related to pain. It also has the ability to measure patient-specific BMD, and potentially monitor BMD changes in individuals prone to OA through longitudinal studies, helping to further explain the role of subchondral bone in the initiation and progression of OA. This research may provide insight into understanding bone-related OA pathophysiology, and may also provide insight into therapeutic targets, such as bone-modifying pharmaceuticals, and improving patient care and pain management.

6.8. Future research

1. For this study, we acquired images of the entire knee joint, including the proximal tibia and the distal femur. CT-TOMASD should be applied to the proximal tibia in this sample to determine if there are regional tibial BMD changes related to pain.
2. The current CT-TOMASD program uses a projection ray technique, limiting it to measuring subchondral BMD at primarily flat or slightly concave surfaces such as the tibia and the patella. The image processing program could be modified to measure BMD patterns at the distal femur, using biplanar reconstruction [129] or curve-detection and surface normal technique permitting for CT-TOMASD analyses for distal femora.
3. We can only hypothesize what the implications of lower BMD, in relation to pain, are related to the mechanical properties of bone. Preliminary finite element (FE) analyses in the proximal tibia showed that trabecular bone has the most dominant effect on structural stiffness [127]. There is a possibility that trabecular bone loss in regions with low BMD may be weak with higher flexibility, possibly leading to pain. We can test this hypothesis through application of finite element (FE) modeling in the patella, to determine how pain may be related to mechanical properties, such as bone strength, stiffness, and deformation, which can be estimated using BMD [7].
4. The current study shows relationships between pain and BMD. We were not able to determine how BMD is affected by OA severity, or if other subchondral regions are affected. To overcome this, images could be collected from a healthy sample to use as a

baseline comparison. This set of normal joint scans could act as an independent variable and could help in possibly determining the causality of pain in relation to BMD.

5. The CT-TOMASD segmenting process in the patella, although less intense than in the tibia, is still time consuming and involves some manual intervention and decision making on the part of the user. By automating the process, we could eliminate some of the subjective decision-making and possibly reduce precision errors [128], especially in peripheral regions. Also, by automating the segmentation process, it may provide more possibility to increase the CT-TOMASD user-base and apply this tool to longitudinal studies.

LIST OF REFERENCES

1. Burr DB. The importance of subchondral bone in the progression of osteoarthritis. Journal of Rheumatology Supplement. 2004 Apr;70:77-80.

2. Radin EL, Paul IL, Rose RM. Role of mechanical factors in pathogenesis of primary osteoarthritis. Lancet. 1972 Mar 4;1(7749):519-22.

3. Burr DB, Schaffler MB. The involvement of subchondral mineralized tissues in osteoarthrosis: quantitative microscopic evidence. Microsc Res Tech. 1997 May 15;37(4):343-57.

4. Radin EL, Rose RM. Role of subchondral bone in the initiation and progression of cartilage damage. Clinical Orthopaedics and Related Research. 1986 Dec(213):34-40.

5. Dieppe P, Lohmander L. Pathogenesis and management of pain in osteoarthritis. The Lancet. 2005;365(9463):965-73.

6. Dieppe P. Subchondral bone should be the main target for the treatment of pain and disease progression in OA. Osteoarthritis and Cartilage. 1999;7(3):325-6.

7. Lammentausta E, Hakulinen MA, Jurvelin JS, Nieminen MT. Prediction of mechanical properties of trabecular bone using quantitative MRI. Physics in Medicine and Biology. 2006;51(23):6187-98.

8. Bellamy N, Buchanan WW, Goldsmith CH, Campbell J, Stitt LW. Validation study of WOMAC: A health status instrument for measuring clinically important patient relevant outcomes to antirheumatic drug therapy in patients with osteoarthritis of the hip or knee. The Journal of Rheumatology. 1988;15(12):1833-40.

9. Felson DT. Clinical practice. Osteoarthritis of the knee. New England Journal of Medicine. 2006 Feb 23;354(8):841-8.

10. Grelsamer RP, Dejour D, Gould J. The Pathophysiology of Patellofemoral Arthritis. Orthopedic Clinics of North America. 2008;39(3):269-74.

11. Neogi T, Felson D, Niu J, Nevitt M, Lewis CE, Aliabadi P, et al. Association between radiographic features of knee osteoarthritis and pain: results from two cohort studies. British Medical Journal. 2009;339:2844-50.

12. Duncan R, Peat G, Thomas E, Wood L, Hay E, Croft P. How do pain and function vary with compartmental distribution and severity of radiographic knee osteoarthritis? Rheumatology. 2008;47(11):1704-7.

13. Gooberman-Hill R, Woolhead G, MacKichan F, Ayis S, Williams S, Dieppe P. Assessing chronic joint pain: Lessons from a focus group study. Arthritis & Rheumatism. 2007;57(4):666-71.

14. Hunter DJ, McDougall JJ, Keefe FJ. The Symptoms of Osteoarthritis and the Genesis of Pain. Rheumatic Disease Clinics of North America. 2008;34(3):623-43.

15. Hannan MT, Felson DT, Pincus T. Analysis of the discordance between radiographic changes and knee pain in osteoarthritis of the knee. The Journal of Rheumatology. 2000;27(6):1513-7.

16. McAlindon TE, Zhang Y, Hannan M, Naimark A, Weissman B, Castelli W, et al. Are risk factors for patellofemoral and tibiofemoral knee osteoarthritis different? Journal of Rheumatology. 1996;23(2):332-7.

17. Duncan RC. Prevalence of radiographic osteoarthritis--it all depends on your point of view. Rheumatology. 2006;45(6):757-60.

18. Duncan R, Peat G, Thomas E, Wood L, Hay E, Croft P. Does isolated patellofemoral osteoarthritis matter? Osteoarthritis and Cartilage. 2009;17(9):1151-5.

19. Buma P. Innervation of the patella: An immunohistochemical study in mice. Acta Orthopaedica Scandinavica. 1994;65(1):80-6.

20. Fortier LA, Nixon AJ. Distributional change in substance P nociceptive fiber patterns in naturally osteoarthritic articulations. The Journal of Rheumatology. 1997;24:7.

21. Burr D. Anatomy and physiology of the mineralized tissues: Role in the pathogenesis of osteoarthrosis. Osteoarthritis and Cartilage. 2004;12:S20-30.

22. Dye SF, Vaupel GL. The pathophysiology of patellofemoral pain. Sports Medicine and Arthroscopy Review. 1994;2:203-10.

23. Johnston JD, Masri BA, Wilson DR. Computed tomography topographic mapping of subchondral density (CT-TOMASD) in osteoarthritic and normal knees: methodological development and preliminary findings. Osteoarthritis and Cartilage. 2009;17(10):1319-26.

24. Johnston JD, Kontulainen SA, Masri BA, Wilson DR. A comparison of conventional maximum intensity projection with a new depth-specific topographic mapping technique in the CT analysis of proximal tibial subchondral bone density. Skeletal Radiology. 2010;39(9):867-76.

25. Johnston JD. Development of a novel non-invasive imaging technique for characterizing subchondral bone mineral density and stiffness. PhD Thesis. Vancouver: University of British Columbia; 2011.

26. Johnston JD, McLennan CE, Hunter DJ, Wilson DR. In vivo precision of a depth-specific topographic mapping technique in the CT analysis of osteoarthritic and normal proximal tibial subchondral bone density. Skeletal Radiology. 2010;40(8):1057-64.

27. Kapandji IA. The Physiology of the Joints: Volume 2 The Lower Limb. 5 ed: Churchill Livingstone; 2002.

28. Ahmed AM, Burke DL, Hyder A. Force analysis of the patellar mechanism. Journal of Orthopaedic Research. 1987;5:69-85.

29. Huberti HH, Hayes WC, Stone JL, Shybut GT. Force ratios in the quadriceps tendon and ligamentum patellae. Journal of Orthopaedic Research. 1984;2:49-54.

30. Hehne HJ. Biomechanics of the patellofemoral joint and its clinical relevance. Clinical Orthopaedics and Related Research. 1990;258:73-85.

31. Heegaard J, Leyvraz PF, Curnier A, Rakotomanana L, Huiskes R. Biomechanics of the human patella during passive knee flexion. Journal of Biomechanics. 1995;28(11):15.

32. Adam C, Eckstein F, Milz S, Putz R. The distribution of cartilage thickness within the joints of the lower limb of elderly individuals. Journal of Anatomy. 1998;193:12.

33. Eckstein F, Muller-Gerbl M, Putz R. Distribution of subchondral bone density and cartillage thickness in the human patella. Journal of Anatomy. 1992;190:425-33.

34. Muller-Gerbl M, Schulte E, Putz R. The thickness of the calcified layer of articular cartilage: a function of the load supported? Journal of Anatomy. 1987;154:103-11.

35. Groll O, Lochmuller EM, Bachmeier M, Willnecker J, Eckstein F. Precision and intersite correlation of bone densitometry at the radius, tibia and femur with peripheral quantitative CT. Skeletal Radiol. 1999 Dec;28(12):696-702.

36. Radin EL, Paul IL. Importance of bone in sparing articular cartilage from impact. Clinical Orthopaedics and Related Research. 1971;78:3.

37. Goldring MB, Goldring SR. Articular cartilage and subchondral bone in the pathogenesis of osteoarthritis. Annals of the New York Academy of Sciences. 2010;1192(1):230-7.

38. Health Canada. Arthritis in Canada: An Ongoing Challenge. Ottawa (ON). 2003. H39-4/14-2003E

39. Lawrence RC, Felson DT, Helmick CG, Arnold LM, Choi H, Deyo RA, et al. Estimates of the prevalence of arthritis and other rheumatic conditions in the United States. Part II. Arthritis Rheum. 2008 Jan;58(1):26-35.

40. Crossley KM, Hinman RS. The patellofemoral joint: the forgotten joint in knee osteoarthritis. Osteoarthritis and Cartilage. 2011;19(7):765-7.

41. Hunter DJ, Zhang YQ, Niu JB, Felson DT, Kwoh K, Newman AB, et al. Patella malalignment, pain and patellofemoral progression: the Health ABC Study. Osteoarthritis and Cartilage. 2007;15:1120-7.

42. Hunter DJ, Harvey W, Gross KD, Felson D, McCree P, Li L, et al. A randomized trial of patellofemoral bracing for treatment of patellofemoral osteoarthritis. Osteoarthritis and Cartilage. 2011;19(7):792-800.

43. Felson DT. The epidemiology of knee osteoarthritis: Results from the Framingham Osteoarthritis Study. Seminars in Arthritis and Rheumatism. 1997;20(3):42-50.

44. Felson DT, Lawrence RC, Dieppe PA, Hirsch R, Helmick CG, Jordan JM, et al. Osteoarthritis: new insights. Part 1: the disease and its risk factors. Annals of Internal Medicine. 2000 Oct 17;133(8):635-46.

45. Dequeker J. Inverse relationship of interface between osteoporosis and osteoarthritis. Journal of Rheumatology. 1997 Apr;24(4):795-8.

46. Hannan MT, Anderson JJ, Zhang Y, Levy D, Felson DT. Bone mineral density and knee osteoarthritis in elderly men and women. Arthritis & Rheumatism. 1993;36(12):1671-80.

47. Elsherif H. Hand osteoarthritis and bone mineral density in postmenopausal women; clinical relevance to hand function, pain and disability. Osteoarthritis and Cartilage. 2008;16(1):12-7.

48. Zhang Y, Hannan MT, Chaisson CE, McAlindon TE, Evans SR, Aliabadi P, et al. Bone mineral density and risk of incident and progressive radiographic knee osteoarthritis in women: The Framingham study. The Journal of Rheumatology. 2000;27(4):1032-7.

49. Bobinac D, Spanjol J, Zoricic S, Maric I. Changes in articular cartilage and subchondral bone histomorphometry in osteoarthritic knee joints in humans. Bone. 2003;32(3):284-90.

50. Hunter DJ, Zhang Y, Niu J, Goggins J, Amin S, LaValley MP, et al. Increase in bone marrow lesions associated with cartilage loss: A longitudinal magnetic resonance imaging study of knee osteoarthritis. Arthritis & Rheumatism. 2006;54(5):1529-35.

51. Lo G, Zhang Y, McLennan C, Niu J, Kiel D, McLean R, et al. The ratio of medial to lateral tibial plateau bone mineral density and compartment-specific tibiofemoral osteoarthritis. Osteoarthritis and Cartilage. 2006;14(10):984-90.

52. Torres L, Dunlop D, Peterfy C, Guermazi A, Prasad P, Hayes K, et al. The relationship between specific tissue lesions and pain severity in persons with knee osteoarthritis1. Osteoarthritis and Cartilage. 2006;14(10):1033-40.

53. Felson DT, Chaisson CE, Hill CL, Totterman SMS, Gale ME, Skinner KM, et al. The association of bone marrow lesions with pain in knee osteoarthritis. Annals of Internal Medicine. 2001;134(7):541-9.

54. Hernandez-Molina G, Neogi T, Hunter DJ, Niu J, Guermazi A, Reichenbach S, et al. The association of bone attrition with knee pain and other MRI features of osteoarthritis. Annals of the Rheumatic Diseases. 2008;67(1):43-7.

55. Brandt KD, Dieppe P, Radin EL. Etiopathogenesis of osteoarthritis. Rheumatic Disease Clinics of North America. 2008 Aug;34(3):531-59.

56. Goldring SR. Role of Bone in Osteoarthritis Pathogenesis. Medical Clinics of North America. 2009;93(1):25-35.

57. Dieppe PA. From protocols to principles, from guidelines to toolboxes: aids to goo management of osteoarthritis. Rheumatology. [Editorial]. 2001;40:841-2.

58. Kellgren JH, Lawrence JS. Radiological assessment of osteo-arthrosis. Annals of Rheumatic Diseases. 1957;16:494-502.

59. Altman RD, Hochberg M, Murphy WA, Jr., Wolfe F, Lequesne M. Atlas of individual radiographic features in osteoarthritis. Osteoarthritis Cartilage. 1995 Sep;3 Suppl A:3-70.

60. Grelsamer RP, Weinstein CH, Gould J, Dubey A. Patellar tilt: The physical examination correlates with MR imaging. The Knee. 2008;15(1):3-8.

61. Hawker GA, Stewart L, French MR, Cibere J, Jordan JM, March L, et al. Understanding the pain experience in hip and knee osteoarthritis - an OARSI/OMERACT initiative. Osteoarthritis and Cartilage. 2008;16:415-22.

62. Woolhead G, Gooberman-Hill R, Dieppe P, Hawker G. Night pain in hip and knee osteoarthritis: A focus group study. Arthritis Care & Research. 2010;62(7):944-9.

63. Bellamy N, Campbell J, Stevens J, Pilch L, Stewart C, Mahmood Z. Validation study of a computerized version of the Western Ontario and McMaster Universities VA3.0 Osteoarthritis Index. The Journal of Rheumatology. 1997 Dec;24(12):2413-5.

64. Stratford PW, Kennedy DM, Woodhouse LJ, Spadoni GF. Measurement properties of the WOMAC LK 3.1 pain scale. Osteoarthritis and Cartilage. 2007;15(3):266-72.

65. Bruyere O, Honore A, Rovati LC, Giacovelli G, Henrotin YE, Seidel L, et al. Radiologic features poorly predict clinical outcomes in knee osteoarthritis. Scandinavian Journal of Rheumatology. 2002;31:13-6.

66. Cicuttini FM, Baker J, Hart DJ, Spector TD. Association of pain with radiological changes in different compartments and views of the knee joint. Osteoarthritis and Cartilage. 1996;4:143-7.

67. Kornaat PR, Bloem JL, Ceulemans RYT, Riyazi N, Rosendaal FR, Nelissen RG, et al. Osteoarthritis of the knee: Association between clinical findings and MR imaging findings. Radiology. 2006;239(3):811-7.

68. McAlindon TE, Cooper C, Kirwan JR, Dieppe PA. Determinants of disability in osteoarthrits of the knee. Annals of the Rheumatic Diseases. 1993;52:5.

69. Draper CE, Fredericson M, Gold GE, Besier TF, Delp SL, Beaupre GS, et al. Patients with patellofemoral pain exhibit elevated bone metabolic activity at the patellofemoral joint. Journal of Orthopaedic Research. 2011;30(2):209-13.

70. Szebenyi B, Hollander AP, Dieppe P, Quilty B, Duddy J, Clarke S, et al. Associations between pain, function, and radiographic features in osteoarthritis of the knee. Arthritis & Rheumatism. 2006;54(1):230-5.

71. Hinman RS, Crossley KM. Patellofemoral joint osteoarthritis: an important subgroup of knee osteoarthritis. Rheumatology. 2007;46(7):1057-62.

72. McWalter EJ, Hunter DJ, Harvey WF, McCree P, Hirko KA, Felson DT, et al. The effect of a patellar brace on three-dimensional patellar kinematics in patients with lateral patellofemoral osteoarthritis. Osteoarthritis and Cartilage. 2011;19(7):801-8.

73. Schultz B, Brown M, Ahmad CS. Evaluation and imaging of patellofemoral joint disorders. Operative Techniques in Sports Medicine. 2010;18:68-78.

74. Merchant AC. Patellofemoral imaging. Clinical Orthopaedics and Related Research. 2001;389:15-21.

75. Chen B, Pei G-x, Jin D, Wei K-h, Qin Y, Qing-si L. Distribution and property of nerve fibers in human long bone tissue. Chinese Journal of Traumatology. 2007;10(1):3-9.

76. Daheshia M, Yao JQ. The bone marrow lesion in osteoarthritis. Rheumatology International. 2010;31(2):143-8.

77. Felson DT, McLaughlin S, Goggins J, LaValley MP, Gale E, Totterman S, et al. Bone marrow edema and its relation to progression of knee osteoarthritis. Annals of Internal Medicine. 2003;139:330-6.

78. Lo GH, McAlindon TE, Niu J, Zhang Y, Beals C, Dabrowski C, et al. Bone marrow lesions and joint effusion are strongly and independently associated with weight-bearing pain in knee osteoarthritis: data from the osteoarthritis initiative. Osteoarthritis and Cartilage. 2009;17(12):1562-9.

79. Yusuf E, Kortekaas MC, Watt I, Huizinga TWJ, Kloppenburg M. Do knee abnormalities visualised on MRI explain knee pain in knee osteoarthritis? A systematic review. Annals of the Rheumatic Diseases. 2010;70(1):60-7.

80. Hunter DJ, Gerstenfeld L, Bishop G, Davis AD, Mason ZD, Einhorn TA, et al. Bone marrow lesions from osteoarthritis knees are characterized by sclerotic bone that is less well mineralized. Arthritis Res Ther. 2009;11(1):R11.

81. Kornaat PR, Kloppenburg M, Sharma R, Botha-Scheepers SA, Graverand M-PH, Coene LNJEM, et al. Bone marrow edema-like lesions change in volume in the majority of patients with osteoarthritis; associations with clinical features. European Radiology. 2007;17(12):3073-8.

82. Dieppe PA, Reichenbach S, Williams S, Gregg P, Watt I, Jüni P. Assessing bone loss on radiographs of the knee in osteoarthritis: A cross-sectional study. Arthritis & Rheumatism. 2005;52(11):3536-41.

83. Simkin PA. Bone pain and pressure in osteoarthritic joints. In: Chadwick DJ, Goode J, editors. Osteoarthritis Joint Pain. Chichester: John Wiley & Sons Ltd.; 2004. p. 179-90.

84. Simkin PA. Pressure-driven Intravasation of Osseous Fat in the Pathogenesis of Osteoarthritic Pain. In: Felson DT, Schaible H-G, editors. Pain in Osteoarthritis. Hoboken, New Jersey: John Wiley & Sons; 2006. p. 175-83.

85. Arnoldi CC, Lemperg RK, Linderholm H. Intraosseous hypertension and pain in the knee. The Journal of Bone and Joint Surgery. 1975;57-B(3):360-3.

86. Bouxsein ML, Seeman E. Quantifying the material and structural determinants of bone strength. Best Practice & Research Clinical Rheumatology. 2009;23(6):741-53.

87. Hochberg MC, Lethbridge-Cejku M, Tobin JD. Bone mineral density and osteoarthritis: data from the Baltimore Longitudinal Study of Aging. Osteoarthritis Cartilage. 2004;12 Suppl A:S45-8.

88. Buckland-Wright C. Subchondral bone changes in hand and knee osteoarthritis detected by radiography. Osteoarthritis and Cartilage. 2004;12:10.

89. Buckland-Wright C. Protocols for precise radio-anatomical positioningof the tibiofemoral and patellofemoral compartments of the knee. Osteoarthritis and Cartilage. 1995;3(Supplement A):71-80.

90. Boegard T, Jonsson K. Radiography in osteoarthritis of the knee. Skeletal Radiology. 1999;28:605-15.

91. McWalter EJ. Links between three-dimensional patellar kinematics, cartilage mophology and varus/valgus alignment in early knee osteoarthritis. MSc Thesis. Vancouver: University of British Columbia; 2004.

92. Bruyere O, Dardenne C, Lejeune E, Zegels B, Pahaut A, Richy F, et al. Subchondral tibial bone mineral density predicts future joint space narrowing at the medial femoro-tibial compartment in patients with knee osteoarthritis. Bone. 2003;32(5):541-5.

93. Clarke S, Wakeley C, Duddy J, Sharif M, Watt I, Ellingham K, et al. Dual-energy X-ray absorptiometry applied to the assessment of tibial subchondral bone mineral density in osteoarthritis of the knee. Skeletal Radiology. 2004;33(10):588-95.

94. Hart DJ, Cronin C, Daniels M, Worthy T, Doyle DV, Spector TD. The relationship of bone density and fracture to incident and progressive radiographic osteoarthritis of the knee: the Chingford Study. Arthritis Rheum. 2002 Jan;46(1):92-9.

95. Nevitt MC, Lane NE, Scott JC, Hochberg MC, Pressman AR, Genant HK, et al. Radiographic osteoarthritis of the hip and bone mineral density. Arthritis & Rheumatism. 1995;38(7):907-16.

96. Lammentausta E, Kiviranta P, Töyräs J, Hyttinen MM, Kiviranta I, Nieminen MT, et al. Quantitative MRI of parallel changes of articular cartilage and underlying trabecular bone in degeneration. Osteoarthritis and Cartilage. 2007;15(10):1149-57.

97. Bennell KL, Creaby MW, Wrigley TV, Hunter DJ. Tibial subchondral trabecular volumetric bone density in medial knee joint osteoarthritis using peripheral quantitative computed tomography technology. Arthritis & Rheumatism. 2008;58(9):2776-85.

98. Burstein D, Hunter DJ. "Why aren't we there yet?" Re-examining standard paradigms in imaging of OA. Osteoarthritis and Cartilage. 2009;17(5):571-8.

99. Leppala J, Kannus P, Natri A, Sievanen H, Jarvinen M, Vuori I. Bone mineral density in the chronic patellofemoral pain syndrome. Calcified Tissue International. 1998;62:548-53.

100. Bayar A, Sarikaya S, Keser S, Ozdolap S, Tuncay I, Ege A. Regional bone density changes in anterior cruciate ligament deficient knees: A DEXA study. The Knee. 2008;15:373-7.

101. Sievanen H, Heinonen A, Kannus P. Adaptation of bone to altered loading environment: a biomechanical approach using X-ray absorptiometric data from the patella of a young woman. Bone. 1996 Jul;19(1):55-9.

102. Murphy E, FitzGerald O, Saxne T, Bresnihan B. Increased serum cartilage oligometric matrix protein levels and decreased patellar bone mineral density in patients with chondromalacia patellae. Annals of the Rheumatic Diseases. 2002;61:981-5.

103. Cann CE. Quantitative CT for determination of bone mineral density: A review. Radiology. 1988;166(2):509-22.

104. UNSCEAR 2000. Report to the General Assembly - Volume 1:Sources and effects of ionizing radiation. United Nations Scientific Committee on the Effects of Atomic Radiation. 2000.

105. UNSCEAR 2000. Report to the General Assembly - Annex B: Exposures from natural radiation sources. United Nations Scientific Committee on the Effects of Atomic Radiation. 2000.

106. Muller-Gerbl M, Putz R, Hodapp N, Schulte E, Wimmer B. Computed tomography-osteoabsorptiometry for assessing the density distribution of subchondral bone as a measure of long-term mechanical adaptation in individual joints. Skeletal Radiology. 1989;18(507-512).

107. Müller-Gerbl M, Putz R, Kenn R. Demonstration of subchondral bone density patterns by three-dimensional CT osteoabsorptiometry as a noninvasive method for in vivo assessment of individual long-term stresses in joints. Journal of Bone and Mineral Research. 1992 Dec;7 Suppl 2:S411-8.

108. Hoechel S, Wirz D, Müller-Gerbl M. Density and strength distribution in the human subchondral bone plate of the patella. International orthopaedics. 2012;36(9):1827-34.

109. Gellert CL, Johnston JD, McLennan CE, Hunter DJ, Wilson DR, editors. In vivo precision of computed tomography topographic mapping of subchondral density (CT-TOMASD) in osteoarthritic and normal patellae. Orthopedic Research Society Annual Conference; 2011.

110. Kontulainen S, Liu D, Manske S, Jamieson M, Sievänen H, McKay H. Analyzing cortical bone cross-sectional geometry by peripheral QCT: comparison with bone histomorphometry. Journal of Clinical Densitometry. 2007;10(1):86-92.

111. Spoor CF, Zonneveld FW, Macho GA. Linear measurements of cortical bone and dental enamel by computed tomography: Applications and Problems. American Journal of Physical Anthropology. 1993;91:469-84.

112. Harris RM. Fractures of the patella and injuries to the extensor mechanism. In: Bucholz RW, Heckman JD, Court-Brown C, editors. Rockwood and Green's Fractures in Adults. 6 ed. Philadelphia: Lippincott, Williams & Wilkins; 2006. p. 1969-97.

113. Glüer CC, Blake G, Lu Y, Blunt BA, Jergas M, Genant HK. Accurate assessment of precision errors: how to measure the reproducibility of bone densitometry techniques. Osteoporos Int. 1995;5(4):262-70.

114. Shrout PE, Fleiss JL. Intraclass correlations: uses in assessing rater reliability. Psychology Bulletin. 1979 Mar;86(2):420-8.

115. Hunter DJ, Felson DT. Osteoarthritis. British Medical Journal. 2006;332(7542):639-42.

116. Burr D. The importance of subchondral bone in osteoarthrosis. Current Opinion in Rheumatology. 1998;10:256-62.

117. Bjurholm A, Kreicbergs A, Brodin E, Schultzberg M. Substance P- and CGRP-immunoreactive nerves in bone. Peptides. 1988;9:165-71.

118. Altman R, Brandt K, Hochberg MC, Moskowitz R, Bellamy N, Bloch DA, et al. Design and conduct of clinical trials in patients with osteoarthritis: Recommendations from a task force of the Osteoarthritis Research Society. Osteoarthritis and Cartilage. 1996;4(4):217-43.

119. Jinks C, Jordan K, Croft P. Measuring the population impact of knee pain and disability with the Western Ontario and McMaster Universities Osteoarthritis Index (WOMAC). Pain. 2002;100:55-64.

120. Milz S, Eckstein F, Putz R. The thickness of the subchondral plate and its correlation with the thickness of the uncalcified articular cartilage in the human patella. Anatomy and Embryology. 1995;192:437-44.

121. Boyd SK, Matyas JR, Wohl GR, Kantzas A, Zernicke RF. Early reginoal adaptation of periarticular bone mineral density after anterior cruciate ligament injury. Journal of Applied Physiology. 2000;89(6):2359-64.

122. Dedrick DK, Goldstein SA, Brandt KD, O'Connor BL, Goulet RW, Albrecht M. A longitudinal study of subchondral plate and trabecular bone in cruciate-deficient dogs with osteoarthritis followed up for 54 months. Arthritis & Rheumatism. 1993;36(10):1460-7.

123. O'Reilly SC, Jones A, Muir KR, Doherty M. Quadriceps weakness in knee osteoarthritis: the effect on pain and disability. Annals of the Rheumatic Diseases. 1998;57:588-94.

124. Burr DR. Muscle strength, bone mass, and age-related bone loss. Journal of Bone and Mineral Research. 1997;12(10):1547-51.

125. Kontulainen SA, Johnston JD, Liu D, Leung C, Oxland TR, McKay HA. Strength indices from pQCT imaging predict up to 85% of variance in bone failure properties at tibial epiphysis and diaphysis. Journal of Musculoskeletal and Neuronal Interactions. 2008 Oct-Dec;8(4):401-9.

126. Shedd KM, Hanson KB, Alekel DL, Schiferl DJ, Hanson LN, Van Loan MD. Quantifying Leisure Physical Activity and Its Relation to Bone Density and Strength. Medicine & Science in Sports & Exercise. 2007;39(12):2189-98.

127. Amini M, Lanovaz J, Szyszkowski W, Johnston JD. Stiffness of the proximal tibial bone in osteoarthritic conditions: A parametric simulation study. Canadian Society of Biomechanics; June 7-10 2012; Vancouver, BC, Canada2012.

128. Kaus MR, Warfield SK, Nabavi A, Black PM, Jolesz FA, Kikinis R. Automated segmentation of MR images of brain tumors. Radiology. 2001;218:586-91.

129. Laporte S, Skalli W, De Guise JA, Lavaste F, Mitton D. A Biplanar Reconstruction Method Based on 2D and 3D Contours: Application to the Distal Femur. Computer methods in biomechanics and biomedical engineering. 2003;6(1):1-6.